Metadata of the chapter that will be visualized in SpringerLink

Book Title	Cognitive Radio Policy and Regulation	
Series Title	4748	
Chapter Title	Case Studies for Advancing CR Deployment	
Copyright Year	2014	
Copyright HolderName	Springer International Publishing Switzerland	
Corresponding Author	Family Name	**Wiecek**
	Particle	
	Given Name	**Dariusz**
	Suffix	
	Division	
	Organization	National Institute of Telecommunications
	Address	Warsaw, Poland
	Email	D.Wiecek@itl.waw.pl
Author	Family Name	**Velez**
	Particle	
	Given Name	**Fernando Jose**
	Suffix	
	Division	Instituto de Telecomunicações–DEM
	Organization	Universidade da Beira Interior
	Address	Covilha, Portugal
	Email	

Abstract	This chapter shows selected practical cases studies dealing with advancing CR deployment. Section 6.1 provides details about TV White Space spectrum estimation methodology based on ITU GE06 Plan rules for cases of countries where high levels of TV interference exist. In addition, an example of addressing the practical co-existence of TV white space devices with incumbent applications in the UHF TV band is presented in this section as well. Section 6.2 looks at the practical possibilities of deploying CR systems in the ISM bands, including a techno-economic viability study of CR solutions in factory scenario. Finally, Sect. 6.3 describes a concept and provides an in depth analysis of using CR technologies in medical environments.

Layout: T1 Standard SC | Book ID: 318863_1_En | Book ISBN: 978-3-319-04021-9
Chapter No.: 6 | Date: 24-12-2013 | Page: 1/40

Chapter 6
Case Studies for Advancing CR Deployment

Dariusz Wiecek and Fernando Jose Velez

Abstract This chapter shows selected practical cases studies dealing with advancing CR deployment. Section 6.1 provides details about TV White Space spectrum estimation methodology based on ITU GE06 Plan rules for cases of countries where high levels of TV interference exist. In addition, an example of addressing the practical co-existence of TV white space devices with incumbent applications in the UHF TV band is presented in this section as well. Section 6.2 looks at the practical possibilities of deploying CR systems in the ISM bands, including a techno-economic viability study of CR solutions in factory scenario. Finally, Sect. 6.3 describes a concept and provides an in depth analysis of using CR technologies in medical environments.

6.1 Utilisation of White Space Devices in TV Bands

6.1.1 Methodology of White Space Estimation in TV Bands Based on ITU GE06 Rules

Dariusz Wiecek

National Institute of Telecommunications, Warsaw, Poland

This section presents methodology of Television White Space (TV WS) estimation taking into account rules for broadcasting services published in the GE06 ITU

D. Wiecek (✉)
National Institute of Telecommunications, Warsaw, Poland
e-mail: D.Wiecek@itl.waw.pl

F. J. Velez
Instituto de Telecomunicações–DEM, Universidade da Beira Interior, Covilha, Portugal

A. Medeisis and O. Holland (eds.), *Cognitive Radio Policy and Regulation*, Signals and Communication Technology, DOI: 10.1007/978-3-319-04022-6_6,

Layout: T1 Standard SC | Book ID: 318863_1_En | Book ISBN: 978-3-319-04021-9
Chapter No.: 6 | Date: 24-12-2013 | Page: 2/40

Agreement [1]. This method was used for preparing maps of TV WS availability in Poland, which were presented originally at COST-TERRA Workshop [2] as well as in CEPT work, which resulted in their inclusion in the ECC Report 185 [3].

6.1.1.1 Introduction

During two sessions of the ITU Regional Radiocommunication Conference RRC'04–RRC'06 technical principles for establishing TV Plans in the VHF and UHF TV bands (174–230 MHz and 470–862 MHz) were prepared. At the RRC Plans for the Digital Terrestrial Television (DTT) Assignments and Allotments were also developed. Rules for changing the Plans and future DTT coordination procedures were written in the GE06 Agreement [1].

Due to lot of incompatibilities between entries in the GE06 Plan (i.e. Assignment and Allotments data planned for inclusion into Plan) many such interference problems were solved by bilateral or multilateral Agreement among interested Administrations. This caused the situation where high interference levels among DTT stations in the UHF band exists in real operational conditions—which cannot be neglected in many countries.

Such "interference limited conditions" (where reception of the DTT should be analysed, taking into account existing interference coming from other DTT stations) is studied and considered, for example during DTT stations coordination procedures between Administrations—when one Administration wishes to include in the Plan new DTT Assignment or change its technical details. Such approach is useful also as a basis of the TV WS availability estimation methodology presented in this chapter.

6.1.1.2 The Methodology

Taking into consideration current UHF TV interference situation, protection requirements can be established by the general GE06 Agreement rules [1] used in case of analysis of new DTT station entry (new planned Assignment in Broadcasting Service). In such situation White Space Device (WSD) can be treated as an additional (much like as new DTT station) transmitter which could be analysed as a "new entry" into the Plan based on the GE06 technical rules. Protection criteria for DVB-T are based on GE06 allotments/assignments parameters (relevant to RN/RPC) for 95 % of location, receiving antenna at 10 m. a.g.l. with directional antenna (for fixed reception) or omnidirectional antenna (for portable receptions). In the analysis, interferences calculations are performed using propagation method ITU-R P. 1546 at 1 % of time 50 % of locations [4]. Aggregate interferences from WSDs should not exceed more than existing interferences from other DTT stations. Such calculation can be performed using GE06 Allotment or Assignment Plan entries data, however it is better to use real operational transmitter characteristics due to fact that such transmissions data can differ from the data written

AQ1

Layout: T1 Standard SC | Book ID: 318863_1_En | Book ISBN: 978-3-319-04021-9
Chapter No.: 6 | Date: 24-12-2013 | Page: 3/40

into Plan. In the case of this section, real calculation of DVB-T transmitter data of all DTT multiplexes in Poland were used, as well as, known technical data of transmitters of neighbouring countries.

In Poland fixed reception type (RPC1 GE06) is used for coverage and interference calculation in case of operational DTT Plans. Taking this into account the technical conditions rules based on the GE06 for calculation were as follows:

- Maximum permissible interfering level at DTT coverage areas: ~ 56 dBmV/m (depending on exact TV channel number, using GE06 field strength corrections);
- Protection Ratio = 21 dB, as defined for GE06 Reference Planning Configuration (RPC1);
- Location probability correction = 13 dB (used for fixed reception RPC1 in case of 95 % of locations);
- Aggregation of WSD interference = 10 dB;
- Receiving antenna discrimination = −16 dB (Fixed antenna discrimination);
- Permissible interfering field strength ~28 dBmV/m in 1 % of time at 10 m a.g.l.

The technical data were used for calculations of size of the buffer zones around DTT service areas generating exclusion areas due to protection of co-channel TV reception. For adjacent N + 1 and N-1 DTT channels the protection areas were the same as the adjacent channels DTT service areas—which means that no adjacent WSDs operations were allowed in the N + 1, N-1 DTT service areas.

6.1.1.3 WSD Channels Availability Calculations Example

TV White Space channels availability calculation based on the methodology presented in the previous subsection was performed. Figure 6.1 shows the calculation done at around 600,000 points (each point of territory within raster of 1 km × 1 km) within whole territory of Poland at UHF frequency range (470–790 MHz). The calculation was performed using the Digital Elevation Map of Poland and neighbouring countries. Protection of all relevant TV transmitters was taken into account.

The colors on the map represent the number of available channels for WSD operation without causing unacceptable interference (for 20 dBm EIRP portable WSD terminal with transmission at 1.5 m a.g.l.). The picture presents one example of such calculations. Further examples can be found in the ECC Report 185 [3].

6.1.1.4 Final Remarks

The methodology presented in this section was used for preparation of the TV WS maps with channels availability for different WSD type configurations and frequency ranges in Poland. Most important results were included in the ECC

Layout: T1 Standard SC | Book ID: 318863_1_En | Book ISBN: 978-3-319-04021-9
Chapter No.: 6 | Date: 24-12-2013 | Page: 4/40

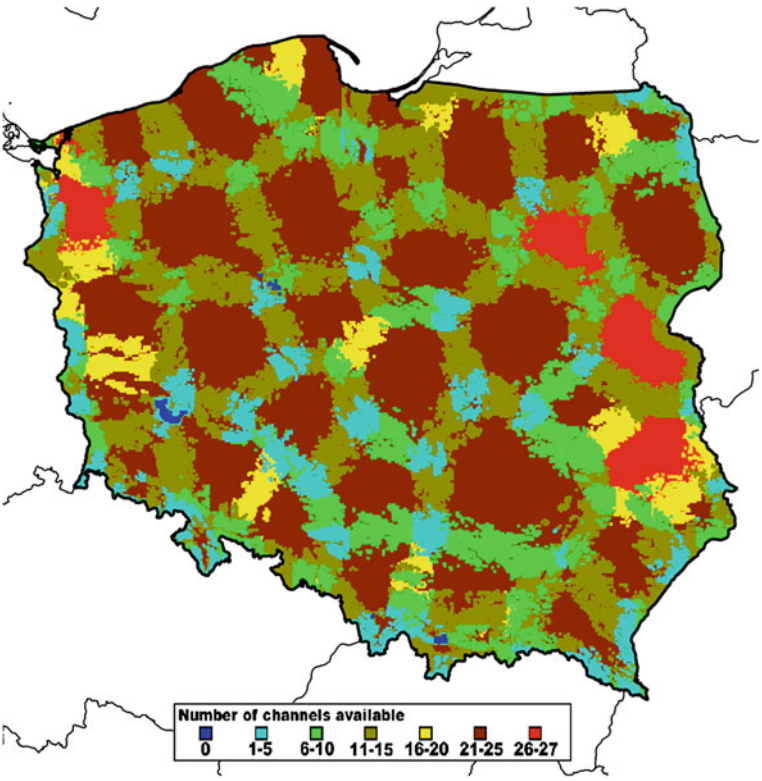

Fig. 6.1 TV white space channels availability calculation at around 600,000 points in Poland

Report [3]. The method could be used also for TVWS channel availability estimation in other GE06 countries (ITU Region 1 and part of Region 3). Required DTT protection level may be established individually in the countries depending on local conditions (DTT type of reception, number of multiplexes, modulation etc.). Such approach is interesting especially in countries where high levels of interference exist which cannot be neglected, i.e. mainly in countries with high-power and high-elevated DTT transmitters.

6.1.2 TVWS Coexistence with Incumbents

Jarkko Paavola,[1] Juha Kalliovaara[2] and Jussi Poikonen[3]

[1] Turku University of Applied Sciences Turku, Finland
[2] University of Turku Turku, Finland
[3] Aalto University Espoo, Finland

Layout: T1 Standard SC | Book ID: 318863_1_En | Book ISBN: 978-3-319-04021-9
Chapter No.: 6 | Date: 24-12-2013 | Page: 5/40

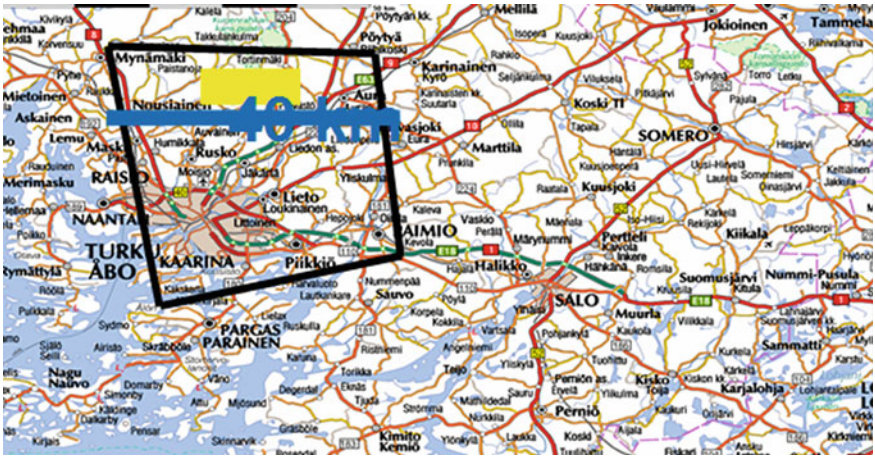

Fig. 6.2 Considered TVWS CR license area

6.1.2.1 Test Environment

A TV White Space (TVWS) test bed has been set up in the WISE project [5], which is part of the Finnish Tekes Trial technology programme [6]. This test bed consists of the following components:

- A commercial level DVB-T test network with three transmitters;
- The Turku University of Applied Sciences radio laboratory equipped with e.g. white space radios, and spectrum analysis and measurement equipment.
- A complementary simulation environment developed by University of Turku and Aalto University.
- A full CR license for the frequency range 470 MHz -790 MHz issued by the Finnish Communications Regulatory Authority (FICORA). This radio license requires a geolocation database to be used to determine available frequencies and maximum transmission power for white space devices operating within the test network. The Turku TVWS testbed utilises a geolocation database maintained by Fairspectrum Ltd.

The CR license of the above outlined test network covers an area of approximately 40 km × 40 km over the Turku region as illustrated in Fig. 6.2.

The test environment has been utilised in interference measurements in order to evaluate maximum transmit power limits for cognitive devices while protecting incumbent operations. Incumbents to be protected in the frequency range 470–790 MHz are TV receivers and PMSE (Programme Making and Special Events) equipment including for example wireless microphone systems.

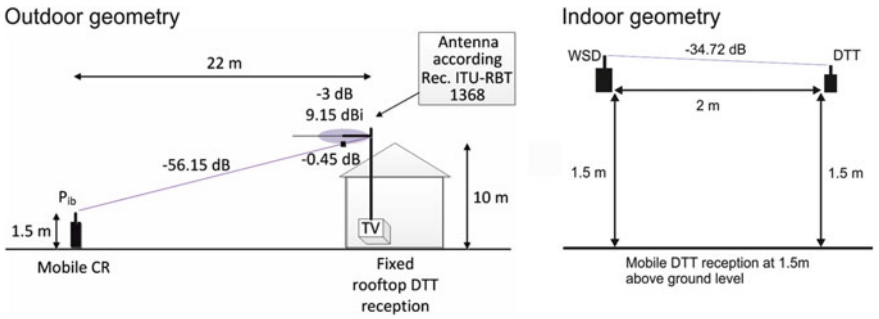

Fig. 6.3 Reference geometries reproduced in the outdoor and indoor measurement campaigns. Adapted from [9]

6.1.2.2 Interference Measurements and Simulations

Measurement campaigns were performed in the TVWS test network to quantify the sensitivity of digital TV reception to interference from nearby WSD devices. Specifically, test TV receivers and WSD transmitters were set up according to outdoor and indoor reference geometries proposed by the ECC [7] to represent worst-case interference scenarios where an interfering WSD is located relatively close to a TV receiver. These geometries are illustrated in Fig. 6.3.

The main objective of the measurements was to determine the protection ratios between received TV signal power and transmitted WSD power. Formally, this ratio was defined as

$$\mathrm{PR}\left(f_{\mathrm{PRI}}, f_{\mathrm{WSD}}\right) = \frac{P_r(f_{\mathrm{PRI}})}{P_{t,\,\max}(f_{\mathrm{WSD}})}$$

that is, the ratio of the received TV signal power centered at frequency f_{PRI} to the maximum allowable power transmitted by the WSD at center frequency f_{WSD}. The maximum WSD transmit power was determined as the limit where error-free TV reception was still possible according to a subjective criterion corresponding approximately to ESR5 [8].

These measurement campaigns were performed with DVB-T and DVB-T2 signal configurations for various DTT receiver locations, signal strengths, and magnitudes of centre frequency separation between the WSD and DTT signals. Detailed descriptions of the measurement setup, scenarios, and numerical results are given in [9–11]. Complementary case studies on distributed sensing algorithms and their effect on secondary system throughput and intersystem interference were conducted using simulation model of the TVWS test network; results of these studies have been presented in [12, 13].

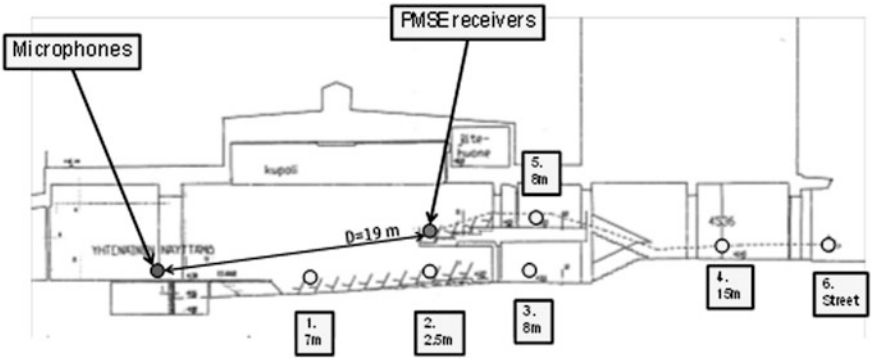

Fig. 6.4 Locations of the PMSE equipment and WSD transmitters measured at the Helsinki City Theatre. Adapted from [14]

6.1.2.3 PMSE Measurements

In addition to DTT receivers, PMSE equipment for example wireless microphone systems operating on the TV White Space frequencies in the lower UHF band also need to be protected from WSD interference. Geolocation databases are currently considered to be the primary method of protecting PMSE users [7]. Sensing techniques are currently not sufficient to provide reliable protection for PMSE [10] and the range of potential deployment scenarios causes large variability in the sensing thresholds [7]. In the following we outline a measurement campaign conducted to evaluate interference between WSD and PMSE devices in a real usage scenario [14].

PMSE equipment was installed into real operating environments in the Helsinki City Theatre. Interference to the PMSE equipment was caused by a simulated WSD operating on the co- or adjacent channel. The measurements were performed with the WSD in several locations inside and outside the building. Figure 6.4 illustrates the location of the microphones and PMSE receivers and the WSD locations (yellow circles) inside the Helsinki City Theatre. Subjective evaluation was used to determine when the WSD were causing audible interference.

The measurements clearly show that a WSD operating co-channel with the PMSE causes interference on very low power levels (−15 dBm … +5 dBm) when the WSD is in the vicinity of the PMSE equipment. Thus, the co-channel operation of PMSE equipment and WSDs is not possible in the vicinity of PMSE receivers. The protection level on the adjacent channel were approximately +30dBm and on the next adjacent channels +40 dBm or more. These values would allow adjacent channel operation with reasonable power levels for the WSDs located close to PMSE equipment.

One approach to manage interference between WSD and PMSE devices is to specify an exclusion zone of certain diameter around the PMSE equipment. WSDs could not operate co-channel with the PMSE equipment when the WSDs are inside the exclusion zone.

Layout: T1 Standard SC | Book ID: 318863_1_En | Book ISBN: 978-3-319-04021-9
Chapter No.: 6 | Date: 24-12-2013 | Page: 8/40

Therefore the PMSE equipment and their locations must be registered to the geolocation database if protection is needed. In the measurements conducted at Helsinki City Theatre it was not possible to cause co-channel interference at a distance of 560 m with the maximum transmit power of approximately 10 W. More detailed studies are still required to reliably estimate the sizes of exclusion zones for PMSE devices.

6.2 CR in ISM Bands

6.2.1 Extracting Interference Information from the ISM/ RLAN bands for CR Applications

John Sydor and Salim Hanna

Communications Research CentreOttawa,ON, Canada

6.2.1.1 Operating CR in the ISM/RLAN Bands

The 2400–2483.5 and 5725–5825 MHz ISM and RLAN bands possesses several attractive features that make them god candidates for CR. The regulatory burden associated with these bands is minimal and there are no licensing fees or licensing requirements for their use. Low-power radio equipment must only meet specific technical requirements to be licence-exempt; some very low-power equipment is even exempt from certification requirements [15, 16].

Spectrum regulators require no or little coordination amongst the different radio systems and devices operating in the ISM/RLAN bands. Therefore most radio applications operate without coordination or coexistence mechanisms, though a few (e.g., Bluetooth and Wi-Fi) are designed to coexist. Thus it is difficult for a radio equipment to perform its tasks without either falling victim or causing harmful interference to or from a multitude of ISM equipment and licence-exempt radio applications such as Wi-Fi (802.11), Bluetooth (802.15.1), ZigBee (802.15.4), video senders, cordless phones, RFID tags, Radars, or medical devices for example.

To make these bands truly attractive for CR, it is imperative that the CR Networks (CRN) working in these bands ascertain the quality of the spectrum and adapt accordingly to mitigate the deleterious effect of uncontrolled, highly varied, interference. Real-time and historical knowledge of the radio environment is needed by CR processes such as Dynamic Spectrum Assignment (DSA) which rely on figures of merit and data that must be extracted from the raw sensed information that the CRN collects. The ISM/RLAN bands are rich in a number of interference metrics, of which a subset can be chosen by the CRN designers in order to create data bases or drive cognitive and adaptive algorithms.

Layout: T1 Standard SC | Book ID: 318863_1_En | Book ISBN: 978-3-319-04021-9
Chapter No.: 6 | Date: 24-12-2013 | Page: 9/40

These metrics can be collected in a number of ways: by co-operative/synchronised sensing, during quiet transmission periods, by designated nodes, etc.; but for ISM and RLAN operation they must be capable of responding to the plethora of diverse interference found in the bands. To achieve these two approaches can be used, either a spectrum analysis/RSSI measurement relying on power or energy detection within a given scanned bandwidth, or by means of monitor-mode receivers capable of responding to the most deleterious class of interference which is typically Wi-Fi based.

6.2.1.2 Power Detection Approaches

Power Spectral Density: Spectrum analysis (SA) has conventionally been used to ascertain radio activity in a band. The process involves measurement of radio signal power within a specific resolution bandwidth (RB), resulting in the creation of a Power Spectrum Density metric. Typically a band is scanned at the RB, a process that usually cannot be carried out at a rate where very rapid (50–500 μs) Wi-Fi packet events are fully captured, thus necessitating multiple scans and integration of readings.

However the process can be simply and cheaply implemented using a common RF radio receive chain, usually with the data demodulation and spectrum analysis processes operating separately because of the requirement of the SA to scan off-channel while the demodulation stays on-channel. The average received power spectral density $PSD(b, s, T)$ from Wi-Fi and non-Wi-Fi signals is measured in bins having (b) (RB) bandwidths over a particular geometric space (s) and a specific period of time (T):

$$PSD(b, s, T) = N^{-1} \sum_{n=1}^{N} psd_n(b, s, T) \tag{6.2.1}$$

where N is the number of measurements over the monitoring period, and $psd_n(b, s, T)$ represents the total received power in the frequency bandwidth b (e.g.; 1 MHz) from DC to the Nyquist sampling rate as captured by the spectrum analyser.

It is noted that this measurement is applicable to the space, s, determined by the capture area of the antenna and that T should be of a sufficiently long integration time to appropriately sample the broadband but transient packet transmissions of the interference. Narrowband PSD analysis is useful primarily for detecting interference sources such as microwave ovens, radars, and video transmitters, which are deleterious sources of interference, necessitating channel changes.

RSSI: The measurement can be obtained by implementing an energy detector of bandwidth b. For detection of Wi-Fi, b is typically 17 MHz. Measurement of the average received signal strength indicator $RSSI(b, s, T)$, of a frequency channel with a bandwidth b over a particular geometric space s and a specific period of time, T, is given by:

$$RSSI(b,s,T) = N^{-1}\sum_{n=1}^{N} rssi_n(b,s,T) \quad (6.2.2)$$

where N is the number of packets captured per channel over the observation period T, and $rssi_n(b,s,T)$ is the received signal strength acquired during receiving an 802.11 packet.

This metric provides an indication of the severity of interference due to the interference on a channel and is useful in qualitatively assessing channel choices; the technique is often used in Wi-Fi routers to provide a channel assessment but provides no information on the frequency or duration of the interference. Readings can be skewed by the occurrence a relatively few and benign high power interference readings over the sampling period, T.

Band RSSI Occupancy: An improved RSSI metric considers occupancy of a band (b) by radio signals over a period of time, allowing a cumulative distribution function (CDF) for the RSSI to be determined. Such a metric can be determined b measurement of the RSSI in a band (b) over a period of time, and determining the intervals at which the RSSI was at or above specific levels. Such data then allows compilation of occurrence (probability) statistics for the RSSI, thus giving cumulative distribution function of the RSSI variable X as the function given by:

$$F_X(x) = P(X \leq x) \quad (6.2.3)$$

where the right-hand side represents the probability that the random variable X takes on a value less than or equal to x. The probability that X lies in the semi-closed interval $(a, b]$, where $a < b$, is then:

$$P(a < X \leq b) = F_X(b) - F_X(a) \quad (6.2.4)$$

The RSSI CDF is a useful channel quality metric as it allows unambiguous comparison of the interference between channels over a common period of time. The implementation of a CDF analyser is slightly more complicated than a RSSI detector, but essentially involves the use of fixed bandwidth RSSI detectors having the standardised Wi-Fi and RLAN channels width (17 MHz). Such detectors are sampled at rates significantly shorter than the smallest expected Wi-Fi packets to create a data base of occurrence statistics. Such detectors typically provide an assessment of the interference caused by Wi-Fi packets only, and the metric can be skewed by narrowband continuous interference (which is best detected by Narrow Band PSD). The CDF statistics shed no information of the packet dimensions or the inter-packet arrival time for the Wi-Fi interference. For such information other approaches need to be used.

6.2.1.3 Monitor-Mode Receivers

Wi-Fi radios with MAC layer software modifications can be highly effective ISM/RLAN band interference detectors. Operating in what is known as a 'monitoring'

mode, IEEE 802.11 signals, including both desired and interference packets are received and processed to extract a number of useful channel interference metrics. Such detectors can share common RF front end receivers and operate separately from the ISM/RLAN band Wi-Fi receivers. In such a manner they can used to scan channels while the data receiver remains fixed on the operating channel.

Interferer Number: Operating in monitor mode allows determination of the unique MAC source addresses of the packets and thus can identify the number of unique transmitters using the channel. The total number of interferers $I(b, s, T)$ captured in a frequency channel with a bandwidth b over a particular geometric space s and a specific period of time T, is given by:

$$I(b, s, T) = M \tag{6.2.5}$$

where M is the total number of unique 802.11 MAC source addresses captured during the observation period T. This metric can be used to assess immediate channel quality, but also provide a metric for the magnitude of potential interference if historical records are kept of the MAC source addresses along with their temporal behaviours.

Packet Duration, Mean Time between Packets: The ability to monitor interference packets allows their frequency of occurrence, duration, and mean time between packets to be determined. Such metrics can be examined as a function of the RSSI, thus allowing determination of threshold levels of interference occurrence; which becomes a useful metric if the desired data link RSSI is known and/or is adjustable. This leads to the notion of channel and band occupancy, which is threshold dependent and can be used to identify the temporal qualities of the interference environment. Some details of how such metrics can be used to provide an enhanced assessment of interference behaviour are given in [17].

Channel Occupancy: A frequency channel with a bandwidth, b, is considered occupied or busy, over a particular geometric space (s) and a specific period of time T, whenever it contains radio frequency energy (due to own activity or emissions from co-channels and adjacent channels within the same system and/or other systems), E, that exceeds a specific threshold, T_o (the threshold is usually taken to be X dB with respect to the noise floor):

$$E(b, s, T) > T_o \tag{6.2.6}$$

Measured channel occupancy, $\varphi(b, s, T)$, can be given by a ratio representing the amount of time, t for which the channel bandwidth is sensed busy over the monitoring period T:

$$\varphi(b, s, T) = t/T \tag{6.2.7}$$

where s is the inner space of locations at which the channel is measured busy. $0 \leq \varphi(b, s, T) \leq 1$ where a value close to zero indicates low activity or channel availability while a value close to unity indicates high activity, potential channel congestion, and performance degradation.

Layout: T1 Standard SC | Book ID: 318863_1_En | Book ISBN: 978-3-319-04021-9
Chapter No.: 6 | Date: 24-12-2013 | Page: 12/40

Band Occupancy: A frequency band representing the union of bandwidths of N adjacent or overlapping channels, $B = U_{n=1}^{N} b_n$, is considered occupied, over the geometric space $S = U_{n=1}^{N} s_n$ and time period T, whenever its ensemble average of channel occupancies exceed a specific threshold T_O:

$$\Phi(B, S, T) = N^{-1} \sum_{n=1}^{N} \phi_n(b, s, T) > T_O \tag{6.2.8}$$

where measured channel occupancies $\varphi_n(s, b, T)$ are determined for all the channels over the same monitoring period T. $0 \leq \Phi(B, S, T) \leq 1$ where a value close to zero indicates spectrum availability while a value close to unity indicates service degradation and potential band congestion.

6.2.1.4 Summary

The ISM and RLAN bands are characterised by a large variety of license-exempt users that create a complex interference environment. Traditional metrics that quantify interference such as RSSI measurement and Spectrum Analysis have defined but limited use in such environments. However, techniques using modified Wi-Fi MAC processes can implement detectors allowing accurate assessments of channel occupancy as a function of time. Such techniques can be used to provide statistics related to interference packet transmission processes and even identify specific interference sources and their activity.

6.2.2 Spectrum Utilisation and Congestion of IEEE 802.11 Networks in the 2.4 GHz ISM Band

Roel Schiphorst and Jan-Willem van Bloem

University of TwenteEnschede, The Netherlands

Wi-Fi technology plays a major role in society thanks to its widespread availability, ease of use and low cost. Many new applications have emerged for such technologies, intelligent transportation systems (ITS), Dynamic Spectrum Access (DSA) systems and offloading of traffic from cellular networks. To assure its long term viability in terms of capacity and ability to share the spectrum efficiently, it is of paramount importance to study the spectrum utilisation and congestion mechanisms in live environments. In the measurements reported in this section we have focused on the crowded 2.4 GHz ISM band. The number of wireless devices (smartphones, laptops, sensors) that use this band is rapidly increasing. In many urban areas not only many WLAN networks can be found, also other systems like Bluetooth, Zigbee and wireless A/V transmission systems use this band.

Layout: T1 Standard SC | Book ID: 318863_1_En | Book ISBN: 978-3-319-04021-9
Chapter No.: 6 | Date: 24-12-2013 | Page: 13/40

On the other hand there is only a limited amount of spectrum available. So it is very likely that interference between systems in this band will occur. Due to the rapid increase of number of wireless devices, interference issue is expected to become even more important. We have addressed this issue by providing a setup to measure the service level—i.e. can all devices fulfil their communication needs—in this band with focus on WLAN standard's amendment IEEE 802.11e (the upcoming IEEE 802.11e is an extension of the 802.11 Wireless Local Area Network (WLAN) standard and is developed to enhance Quality of Service (QoS) support).

Researching spectrum utilisation and congestion in 802.11 networks is important for CR in the broad sense, as many CR implementations are based on 802.11 technologies, but translated to a different frequency band. An example being the 802.11af extension for white spaces in TV bands [18]. Identifying bottlenecks in 802.11 can be therefore used to enhance throughput and QoS which is especially relevant in the heterogeneous environments where CR is often used.

In this research, a cross-layer approach is used [19], since the service level can be measured at several levels of the protocol stack. The focus is on monitoring at both the Physical (PHY) and the Medium Access Control (MAC) link layer simultaneously by performing respectively power measurements with a spectrum analyser to assess spectrum utilization and packet sniffing to measure the congestion. Compared to traditional QoS analysis in 802.11 networks, packet sniffing allows studying the occurring congestion mechanisms more thoroughly. The measurement equipment consists of:

- Packet sniffer: to capture raw packets on MAC link layer level;
- RF monitoring equipment: spectrum analyser tuned to the 2.4 GHz ISM band.

The monitoring was applied for the following two cases. First the influence of interference between WLAN networks sharing the same radio channel was investigated in a controlled environment. It turned out that retry rate, Clear-To-Send (CTS), Request-To-Send (RTS) and (Block) Acknowledgment (ACK) frames can be used to identify congestion, whereas the spectrum analyser may be employed to identify the source of interference. Secondly, live measurements were performed at three locations to identify the type of interference in real situations.

Below we describe the results of live measurements in more detail. Figure 6.5 shows the mean number of frames per second per location. It has been split up into management, control, data and retry frames. First of all the results show that the college room location has most traffic which is due to measurements that were carried out at a college area with 75 to 100 students. Secondly, in this location about 70 % of the captured traffic were control frames and only about 21 % where the actual data traffic. The sub-field identifiers reveal that most of the control frames are RTS, CTS and, to a lesser extent, ACK and Block ACK packets. This is in line with the lab experiments where the same type of control frames have been shown to identify congestion.

The measurements carried out in a college are most interesting and reviewed below in more detail. Figure 6.6 shows the observed RF spectrum. From Fig. 6.7 it can be seen that the WLAN traffic is very spiky as expected. These measurements

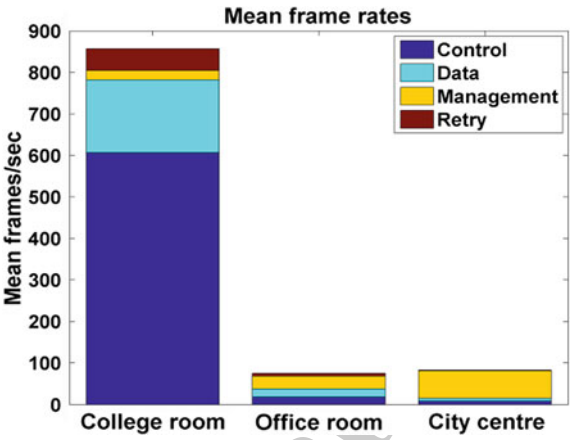

Fig. 6.5 Occurrence of different packet types

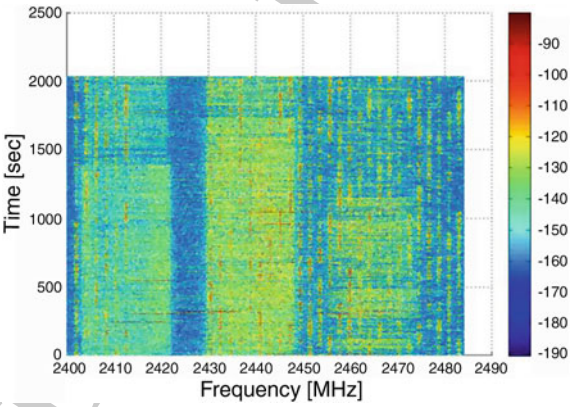

Fig. 6.6 RF spectrum in the college room

were performed during a college classes being in session until the time corresponding to 1400 s mark in scales of Figs. 6.6 and 6.7.

It may be noted that when the classes ended at 1400 clock mark, a sharp downwards transition is observed in the RF channel occupancy of Fig. 6.6. Moreover, at this particular moment the occupancy drops from values around 65–20 %.

6.2.2.1 Conclusion

Our measurements revealed that there is severe performance degradation in 802.11 networks in scenarios with many users, i.e. in situations where capacity is most needed. Especially the performance of the MAC layer based on CSMA/CD (Carrier Sense Multiple Access/Collision Detection) degrades in these scenarios; decreasing the throughput of data packets to less than 25 % of all packets. Similar performance degradations can be expected by CR applications based on 802.11

AQ2

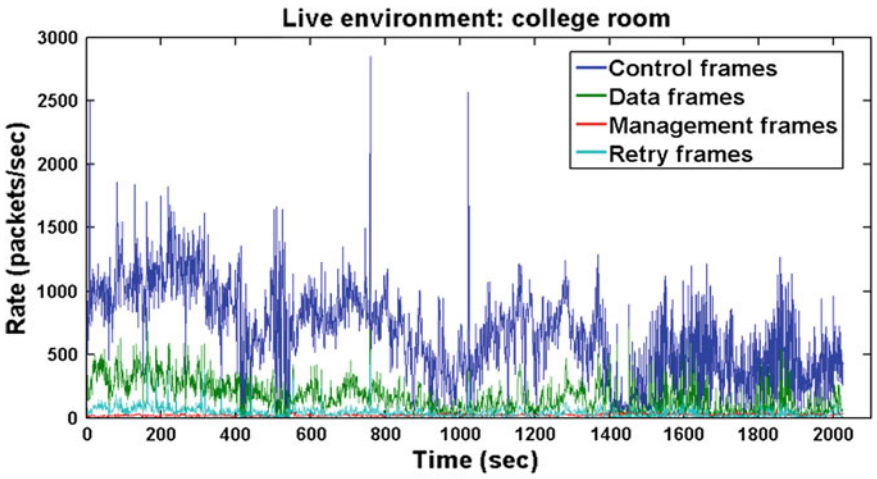

Fig. 6.7 Packet rate for the different MAC packet types versus time in the college room

technology. Further research should focus on improving the performance, an example being oCSMA (optimal CSMA) [20].

6.2.3 Techno-Economic Viability of Cognitive Solutions for a Factory Scenario

Vânia Gonçalves[1] and Lieven Tytgat[2]

[1] iMinds–SMIT Vrije Universiteit Brussel Brussels, Belgium
[2] iMinds–IBCN Ghent University Ghent, Belgium

Wireless and mobile applications are projected to grow by orders of magnitude in the coming years. While the number of devices explodes, so do their application domains. These different application domains have specific needs, which are tackled by an ever-increasing amount of different technologies. The major concern arising is that a number of these technologies use the same limited spectrum, even though they have not been designed to coexist with one another, resulting in a severe degradation of the operation of these networks. Dynamic Spectrum Access (DSA) promises to alleviate most of the coexistence problems between different technologies. However, DSA economic and business feasibility is still to be recognised by concrete results showing economic gains. In this section we hypothesise about how valuable could DSA be in indoor settings. Towards this goal, different implementation alternatives of spectral sensing engines within an industrial context are assessed and the trade-off between the added cost and the increased usability of coexisting IEEE 802.11 and IEEE 802.15.4 networks is identified.

When considering actual deployment of DSA in real-life, there is a natural techno-economic trade-off between benefit and cost. We focus on an industrial plant where a ZigBee based wireless sensor network monitors and controls the production equipment, while WLAN provides wireless access to the data network of the plant. Within such an environment Wi-Fi and ZigBee coexist in the unlicensed ISM band. The economic benefit of implementing DSA on top of regular ZigBee and Wi-Fi is the reduction of machine failure rate and production disruption. An added cost will arise due to the actual implementation cost of the selected solution and increased cost of battery replacement due to the shortened battery lifetime.

6.2.3.1 Business Scenario

A modern electronics contract manufacturer that operates multiple Surface Mount Technology (SMT) assembly lines is the focus of our scenario. A mid-size manufacturer may operate a production floor with 15 assembly lines in parallel. Each line includes 3–4 robots and one oven, and is constantly monitored by 2 human operators on the production floor. Each robot contains 2 cameras and 6–7 different ZigBee sensors, while the ovens contain another 10 ZigBee sensors each, bringing the total number of ZigBee sensors throughout the production floor to 600. These sensors form a ZigBee wireless sensor and actuator network (WSAN). They measure the temperature and other parameters of machinery and processes on the assembly line, and transmit it periodically to a central control and monitoring system. This system alerts human operators of various types of malfunctions, e.g. component-feed problems and overheating, which typically happen multiple times every day.

The wireless LAN in the factory is composed of 100 Wi-Fi devices, including access points, laptops, portable terminals and smartphones. For example, each of the operators of the assembly lines has a portable terminal that he uses to control software download to the assembly machines, verify that proper material is loaded in the robots, etc. Since the sensors are located to monitor critical parameters in the assembly lines, loss of ZigBee data might lead to severe damage to machinery and significant loss of material. Two types of failure are possible. Major Failures are ones that risk damage to machinery. If, for example, a machine overheats while ZigBee packets are lost, the supervisors will not be alerted in time, which could lead to serious damage to the machine and a full stop of the assembly line until the damage is repaired. This would reduce production output, and decrease revenue as a result. Minor Failures are ones that only risk loss of material and profit. If, for example, one of the SMT component feeders gets jammed, then all products that continue to be produced before the problem is fixed are damaged, and considered lost. In our scenario each assembly line uses $700 worth of materials and produces $300 of profit per hour of uninterrupted operation. We assume that every assembly line develops conditions that, if not detected on time, will cause a Major Failure

Layout: T1 Standard SC | Book ID: 318863_1_En | Book ISBN: 978-3-319-04021-9
Chapter No.: 6 | Date: 24-12-2013 | Page: 17/40

once every year. We also assume that, on average, every assembly line suffers a Minor Failure once every hour. Furthermore, we estimate that an assembly line that suffers a Major Failure will shut down for 24 h, and the total cost of repair, in labour, equipment and replacement parts, is $10,000. We also estimate that if a Minor Failure occurs while ZigBee packets are lost, it will take additional 30 s to detect the failure and stop production.

Due to the substantial opportunity costs and repair costs, it is clear that the factory owner is interested in reducing interference to an acceptable minimum. Therefore, we propose the solution of adding cognitive elements to the wireless devices. These come however at an investment cost that must be balanced with the performance gains they promise to deliver. We compare over a 5-year period a reference Scenario 1 of a factory with standard Wi-Fi and ZigBee networks and no cognitive solutions, to three alternative set-ups: Scenario 2 consists of deploying a sensing engine on ZigBee devices; Scenario 3 with sensing engines deployed in Wi-Fi devices; and Scenario 4 with sensing engines deployed in both ZigBee and Wi-Fi devices.

6.2.3.2 Potential Benefits

Sensing reduces the interference between the ZigBee and Wi-Fi networks. In fact, sensing therefore reduces the amount of machinery and assembly line failures, which are caused by late alerting due to interference. The economic gains of sensing are thus derived from the amount of failures (along with their costs and losses) that can be avoided. These failures can, as mentioned in the scenario description, be divided into two groups. In the absence of any monitoring sensors, Major failures would occur on average once a year on each line. With a total cost of $1.290.000 over 5 years, Major failures represent a very large potential loss for the factory. Again, in the absence of any monitoring sensors, Minor failures would occur on average once an hour on each line and would account to $5.475.000 over 5 years, representing even a larger potential loss than Major failures. In summary, the potential total cost of failures in 5-years-time amounts up to $6.765.000. This significant figure is the reason monitoring sensors are indeed deployed in assembly lines and other industrial plants.

6.2.3.3 Potential Costs

The additional investment cost comes down to the extra price of a node that is equipped with a sensing engine. The core of this engine is an Application Specific Integrated Circuit (ASIC), of which the cost is estimated at $1. Within a Wi-Fi device, no additional components need to be added and therefore we estimate the cost of one sensing engine for a Wi-Fi device at $1. For ZigBee sensors it is necessary to add additional components. We estimate the total cost of this sensing engine at

Layout: T1 Standard SC | Book ID: 318863_1_En | Book ISBN: 978-3-319-04021-9
Chapter No.: 6 | Date: 24-12-2013 | Page: 18/40

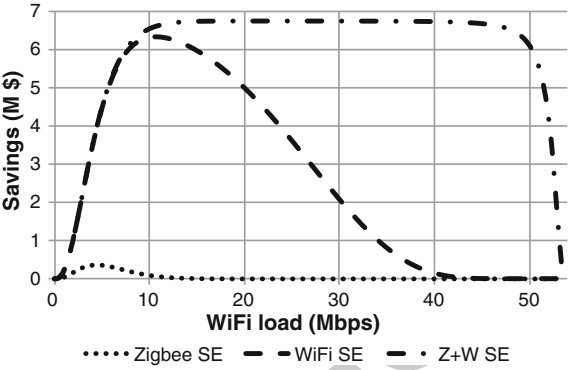

Fig. 6.8 Savings due to implementation of sensing as function of average Wi-Fi load over a 5-year period

$10. Because there are 600 ZigBee nodes and 100 Wi-Fi devices throughout the factory, we estimate the total additional investment in Scenario 2 at $6.000, in Scenario 3 at only $100 and in Scenario 4 at the sum of these 2 cases, $6.100.

6.2.3.4 Conclusions

Figure 6.8 presents the total expected savings due to the implementation of sensing engines compared to no sensing. Scenario 2 (ZigBee SE) presents little savings in a very small Wi-Fi load range. Scenario 3 (Wi-Fi SE) shows high savings under most common Wi-Fi loads, while Scenario 4 (Wi-Fi and ZigBee SE) presents high savings under all real-world Wi-Fi loads.

The costs due to machine failure in this setting are limited to only $1K at 28.6 Mbps, $10K at 38.5 Mbps and $100K at 46 Mbps average Wi-Fi load during a 5-year period. By effectively limiting the costs, the savings are thus the highest for a scenario in which the sensing engine is implemented in both Wi-Fi and ZigBee. This is a consequence of the high reliability, for low as well as high Wi-Fi loads. Although this analysis is within a certain factory scenario, its results can be extrapolated towards different settings where reliability of the ZigBee network is needed.

Acknowledgments: The research leading to these results has received funding from the European Union's Seventh Framework Programme FP7/2007-2013 under grant agreements n° 257542 (CONSERN project) and n° 258301 (CREW project). It has also received funding from IWT under projects ESSENCES and WINETS2020. Contributions from colleagues and project partners are here acknowledged, with special contribution from Matthias Barrie.

Layout: T1 Standard SC | Book ID: 318863_1_En | Book ISBN: 978-3-319-04021-9
Chapter No.: 6 | Date: 24-12-2013 | Page: 19/40

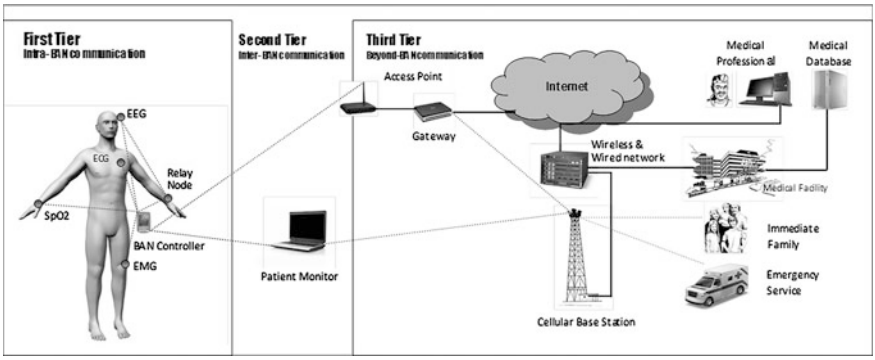

Fig. 6.9 Three-tier architecture of a telemedicine system

6.3 CR in Medical Environments

Raúl Chavéz-Santiago[1], Norberto Barroca[2], Fernando J. Velez[2], Ilangko Balasingham[1], Henrique M. Saraiva[2], Paulo T. Gouveia[2], Jorge Tavares[2] and Luis M. Borges[2]

[1] Oslo University Hospital Norwegian University of Science and Technology Trondheim, Norway
[2] Instituto de Telecomunicações–DEM Universidade da Beira Interior Covilha, Portugal

6.3.1 Introduction

Wireless communications have the potential to impact beneficially medical practice through the development of ubiquitous health monitoring solutions [21, 22]. This can be achieved through the use of biomedical sensors combined with small wireless intercommunicating radio transceivers for measuring, transmitting, and storing different physiological signals in real time. The interconnection of these wearable and implantable devices constitutes a body area network (BAN), which is the core of modern telemedicine systems (Fig. 6.9).

A dedicated frequency band in 2360-2400 MHz for BAN use on a secondary basis has recently been designated in the United States. Nevertheless, it is anticipated that a large number of wireless biomedical sensors will operate in unlicensed frequency bands too. In fact, the BAN IEEE 802.15.6 standard [23] has recommended the unlicensed 2.4 GHz industrial, scientific, and medical (ISM) frequency band in 2400–2500 MHz and ultra wideband (UWB) in 3.1–10.6 GHz as alternative spectrum for wireless biomedical sensors. Small transceivers compliant with the IEEE 802.15.4 (ZigBee) standard are commercially available for operation in unlicensed ISM bands and have been found suitable for health and fitness monitoring in confined indoor areas [24]. In addition, a large number of

Layout: T1 Standard SC | Book ID: 318863_1_En | Book ISBN: 978-3-319-04021-9
Chapter No.: 6 | Date: 24-12-2013 | Page: 20/40

wireless local area networks (WLAN) based on the family of IEEE 802.11 standards also share the 2.4 GHz ISM band, making the coexistence of these different wireless devices challenging [25]. Similar interference scenarios may be expected in the UWB band [26]. Techniques to avoid mutual interference must be applied in such cases. In hospital scenarios, the coexistence problem is more critical in small areas like intensive care units (ICUs) and operating rooms (ORs) because electromagnetic interference (EMI) from wireless devices can disrupt the performance of non-communication medical equipment that is routinely present in such premises. CR is a promising technology that can ease the coexistence of wireless devices while protecting the electronic medical equipment. Despite the recognized potential benefits of CR for BANs [27], this application has not been extensively investigated and just a few solutions have been proposed.

Future improvements in radio frequency (RF) energy harvesting technology will facilitate the creation of a network with no need of dedicated transmitters, as a reliable source of wireless energy power [28]. This can be accomplished by enabling the capture of electromagnetic energy from multiple available ambient RF energy sources, such as mobile base stations, TV and radio transmitters, microwave radios, and mobile phones. Moreover, since wireless body area network (WBAN) nodes are battery operated, energy recharging is a possibility, avoiding the need of battery replacement. However, the service lifetime of the electronic components could be a major concern if there is no possibility to collect enough energy to generate the voltage needed to drive the sensor node. Medium access control (MAC) and routing protocols also play an important role in the network performance [29]. As a consequence, choosing the best opportunities poses a high effect on the overall network performance, as well as on the energy consumption.

The WBAN MAC protocols are responsible for providing the mechanisms for scheduling and allocation of the shared wireless channel. Compared to conventional WBANs, the MAC layer of WBAN nodes with CR capabilities must handle additional challenges, such as silent spectrum sensing periods and the need for high priority access mechanisms, for the distribution of spectrum sensing and decision results [30]. Therefore, the new innovative MAC protocols must be design regarding energy efficiency.

IEEE 802.15.4 has become the de facto standard for Wireless Sensor Networks (WSNs) being used in a wide range of scenarios and applications. The associated MAC protocol is responsible for triggering the current transmission allowing for multiple sensor nodes to share the same communication medium as well as to determine and change the operation mode of the radio transceivers whilst saving energy.

Layout: T1 Standard SC | Book ID: 318863_1_En | Book ISBN: 978-3-319-04021-9
Chapter No.: 6 | Date: 24-12-2013 | Page: 21/40

6.3.2 Hospital Scenarios

CR has been identified as the enabling technology to tackle spectrum scarcity and interference in healthcare and medical telemetry by enabling dynamic utilization of the wireless medical telemetry services (WMTS) frequency band, which comprises different parts of the spectrum, namely 608–614, 1395–1400, and 1427–1432 MHz [31]. A CR request-to-send/clear-to-send (RTS/CTS) protocol for e-health applications was proposed in [32], which adapts the transmit power of wireless devices operating in 2.4 GHz according to standardized electromagnetic immunity (EMI) constraints. The protocol effectively handles two different types of medical application traffic with different priorities. Through computer simulations it was demonstrated that this EMI-aware RTS/CTS protocol can reduce significantly the interference to protected non-communication medical devices in comparison to other medium access control (MAC) protocols like the specified by IEEE 802.15.4. Finally, a CR solution for BAN based on ultra wideband (UWB) technology was proposed in [33]. UWB signals offer many advantages to BANs, and some features of this technology can be exploited for effective implementation of CR. Below, the two latter approaches, namely CR for BAN in 2.4 GHz and UWB bands, are described with more detail.

6.3.2.1 Cognitive Radio Solution in 2.4 GHz

In the hospital case study in [32], two different types of traffic from two wireless e-heath applications were considered to be handled by the CR system:

(1) Real-time non-critical telemedicine, which is used to transmit data that are not delay/loss-sensitive, e.g., remote consultation, patient record transfers, and remote diagnosis.

(2) Hospital information system, which collects patient, technical, and facility data that are intended for better clinical decisions and to prevent patient complications. This system collects information with the aid of BANs and other wireless sensor networks (WSNs) located in the hospital.

In the CR context, the telemedicine system is treated as primary user (PU) and the hospital information system as secondary user (SU).

The CR system consists of three components, namely an inventory system, a CR controller (CRC), and CR clients. The inventory system is a database containing information about all the medical devices in the hospital premises. Information like location, activity status, and EMI immunity levels are stored in the database. The CRC is a computer that controls the transmission parameters of the CR clients, i.e., PUs and SUs. For this sake, the CRC uses the information in the inventory system to compute the appropriate transmit power for each CR client in order to avoid interference that exceeds the EMI immunity levels of non-communication medical devices located in the vicinity. The CR system operates using a dedicated control channel (DCC) and a data channel (DATC). Both channels are

Layout: T1 Standard SC | Book ID: 318863_1_En | Book ISBN: 978-3-319-04021-9
Chapter No.: 6 | Date: 24-12-2013 | Page: 22/40

in unlicensed spectrum, e.g., the 2.4 GHz ISM band. Every CR client transmits its data through the CRC. The CRC can transmit/receive data from both channels simultaneously, whereas the CR clients can transmit just in one of the two channels at a time. The DCC is used to broadcast information to all the CR clients about their corresponding maximum power, P_{ctrl}, for transmitting RTS messages. Each CR client has a different P_{ctrl} value depending on its location, and it is calculated as

$$P_{\text{ctrl}} = \min\left\{\min_{n}(P_{\text{NLS}}(n)), \min_{m}(\text{P}_{\text{LS}}(m))\right\} \tag{6.3.1}$$

where $P_{\text{NLS}}(n)$ and $P_{\text{LS}}(m)$ are the upper bounds on transmit power for non-life-supporting (NLS) medical device n and life-supporting (LS) medical device m, respectively. For a frequency range of 800–2500 MHz, these transmit power values can be computed as:

$$P_{\text{NLS}}(n) = \left(\frac{D_{\text{NLS}}(n)E_{\text{NLS}}(n)}{7}\right)^2 \tag{6.3.2}$$

and

$$P_{\text{LS}}(m) = \left(\frac{D_{\text{LS}}(m)E_{\text{LS}}(m)}{23}\right)^2 \tag{6.3.3}$$

where $D_{\text{NLS}}(n)$ and $D_{\text{LS}}(m)$ are the distance from the CR client to the NLS device n and LS device m, respectively; $E_{\text{NLS}}(n)$ and $E_{\text{LS}}(m)$ are the EMI immunity levels for the NLS and LS medical devices n and m, respectively, the values of which are stored in the inventory system.

Since the protected non-communication medical devices can be turned ON or OFF and the locations of the CR clients change dynamically, P_{ctrl} must be computed and broadcasted every t_p slots on the DCC. All the transmissions from CR clients are paused during broadcasting of P_{ctrl} to synchronize with the CRC.

In order to access the channel, a CR client transmits a RTS message to the CRC on the DCC. If a collision occurs, the colliding CR clients wait for a random time based on a constant back-off window for PUs and exponential back-off window for SUs. The CR clients can retransmit the RTS message with probability α_1 for PUs and α_2 for SUs. A limited number of SUs can be in a queue, referred to as the imaginary orbit, waiting for retransmission, whereas this number is unlimited for PUs. When a RTS is successfully received by the CRC, the maximum transmit power on the DATC, P_{data}, is computed in the same way as P_{ctrl}. If the CRC cannot find a suitable transmit power that satisfies the minimum quality of service (QoS) of the CR client without violating the EMI constraints given by either (6.2.2) or (6.2.3), the request for data transmission is dropped. In addition, the CRC randomly drops RTS messages with probability P_{d1} for PUs and P_{d2} for SUs in order to avoid network congestion. If the CR client's RTS is dropped, a negative-CTS message is sent by the CRC; after a random number of time slots the CR client can

Layout: T1 Standard SC | Book ID: 318863_1_En | Book ISBN: 978-3-319-04021-9
Chapter No.: 6 | Date: 24-12-2013 | Page: 23/40

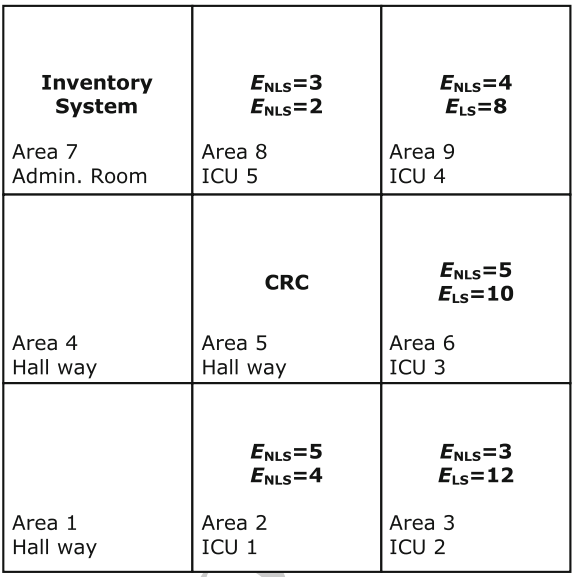

Fig. 6.10 Layout of hospital scenario used for simulations

attempt to transmit again. If the CR client is not dropped, then a CTS message is sent. After the CTS message is successfully received, the CR client will wait in a transmission queue of finite size, which means the CR client's request will be dropped if the queue is full. PUs and SUs wait in separated queues, and PUs always have priority to transmit on the DATC. The number of time slots for data transmission is geometrically distributed with parameters β_1 and β_2 for PUs and SUs, respectively.

6.3.2.2 Performance Evaluation

The EMI-aware protocol described above can be evaluated through numerical simulations in terms of interference probability and outage probability [32]. For performance comparison with a traditional MAC protocol, a scenario consisting of hospital premises over 27 m^2 arranged in nine areas of equal size comprising a hall way, an administration room, and five ICUs were used, as shown in Fig. 6.10.

In this case study, the CRC was located at the center of area 5. Ten NLS and LS non-communication medical devices were located in the ICUs, and their corresponding EMI immunity levels are also given in Fig. 6.10. The locations of the NLS and LS medical devices and the CRC were fixed, whereas the CR clients were mobile and uniformly distributed over the area. A random pedestrian mobility model mimics the wandering of the CR clients. In order to compute (6.3.2) and (6.3.3), the following indoor path loss (PL) formula as a function of the distance in meters, d ($d > 1$), was applied:

Layout: T1 Standard SC | Book ID: 318863_1_En | Book ISBN: 978-3-319-04021-9
Chapter No.: 6 | Date: 24-12-2013 | Page: 24/40

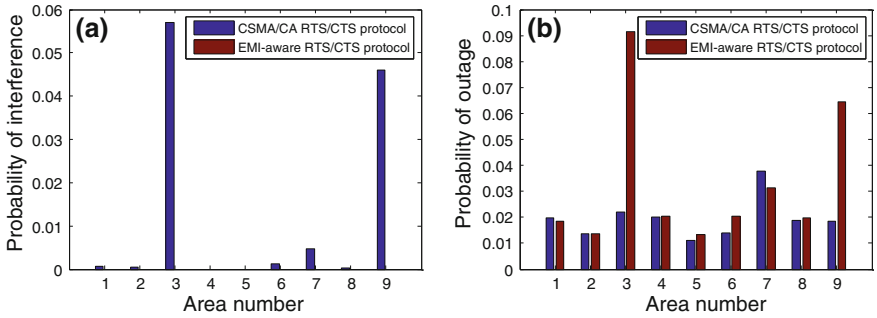

Fig. 6.11 **a** Interference probability and **b** outage probability over the nine areas of the hospital scenario

Fig. 6.12 Outage probability over the nine areas of the hospital scenario for different multiband EMI-aware RTS/CTS protocols

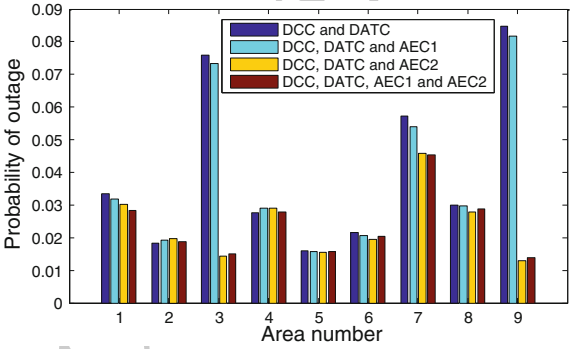

$$\mathrm{PL}_{\mathrm{total}} = 37.7 + 3.3\log_{10}(d) + 16.2n \tag{6.3.4}$$

where n is the number of floors (or walls) the radio signal has to traverse and PL is given in decibels (dB).

The interference probability was defined as the chance that a wireless CR client causes interference to the non-communication medical devices by violating (6.3.2) or (6.3.3). In the EMI-aware RTS/CTS protocol, interference occurs when the ON status of the medical devices is reported wrongly to the CRC. This probability of misdetection was set to 0.01.

The interference probabilities of each area for the EMI-aware RTS/CTS protocol and a traditional carrier sense multiple access with collision avoidance (CSMA/CA) RTS/CTS protocol are shown in Fig. 6.11a.

As may be observed, the EMI-aware RTS/CTS protocol successfully protected NLS and LS medical devices. The outage probability, i.e., the probability that the received signal strength at the CRC is less than −65 dBm, is depicted in Fig. 6.11b for each of the nine areas. Evidently, the interference reduction comes at the expense of high outage probability for the wireless devices in areas where protected medical equipment are located.

6.3.2.3 Enhancement Through the Use of an Additional Channel

The EMI-aware RTS/CTS protocol in [32] can be enhanced by including dual-band operation [34]. The use of an additional "emergency" channel (AEC) in a different frequency band that can serve as a control/data channel for potential interferers can reduce the outage probability. The recently allocated 2360-2400 MHz BAN frequency band and the 900 MHz ISM band (902–928 MHz) are suitable for allocation of the AEC. Through computer simulations, the performance of this MAC scheme was evaluated in terms of the outage probability, and the comparison with the EMI-aware RTS/CTS protocol in [32] is depicted in Fig. 6.12.

Clearly, the use of an AEC reduced the outage probability, but the improvement is determined by the center frequency of the AEC. Marginal improvement is obtained with an AEC in 2360–2400 MHz (AEC1), whereas significant improvement can be obtained by using an AEC in the 900 MHz ISM band (AEC2). The simultaneous use of AEC1 and AEC2 does not provide further improvement.

6.3.2.4 Cognitive Radio Solution in the UWB Band

Besides large bandwidth that enables high data rate transmission, UWB technology has other attractive characteristics for BAN implementation. UWB signals have an inherent noise-like behavior due to their extremely low maximum effective isotropically radiated power (EIRP) spectral density of –41.3 dBm/MHz. This makes UWB difficult to detect and increases its robustness against jamming, potentially rescinding the need for complex encryption algorithms in small, low-cost transceivers. In addition, compared to single-band orthogonal frequency division multiplexing (OFDM) where symbols are continually sent on one frequency band, for multiband OFDM (MB-OFDM), symbols are interleaved over multiple sub-bands across both time and frequency. By interleaving the OFDM symbols across sub-bands in this manner, multiband UWB can maintain the power level associated with a single-band OFDM transmission yet the data throughput can be significantly increased. MB-OFDM UWB technology can currently achieve rates ranging from 53.3 to 480 Mbps over distances up to 10 m.

Additionally, UWB signals do not represent a threat to patients' safety and are not significant sources of interference to other medical devices. Impulse radio (IR) UWB transceivers have a simple structure and very low power consumption characteristics. These features facilitate their miniaturization for wearable biomedical sensors.

6.3.2.5 Architecture of a Cognitive Radio Controller for BAN

Characteristics of UWB technology can be exploited to turn a BAN controller into a CR controller (CRC). The CRC is a central unit that controls the transmission

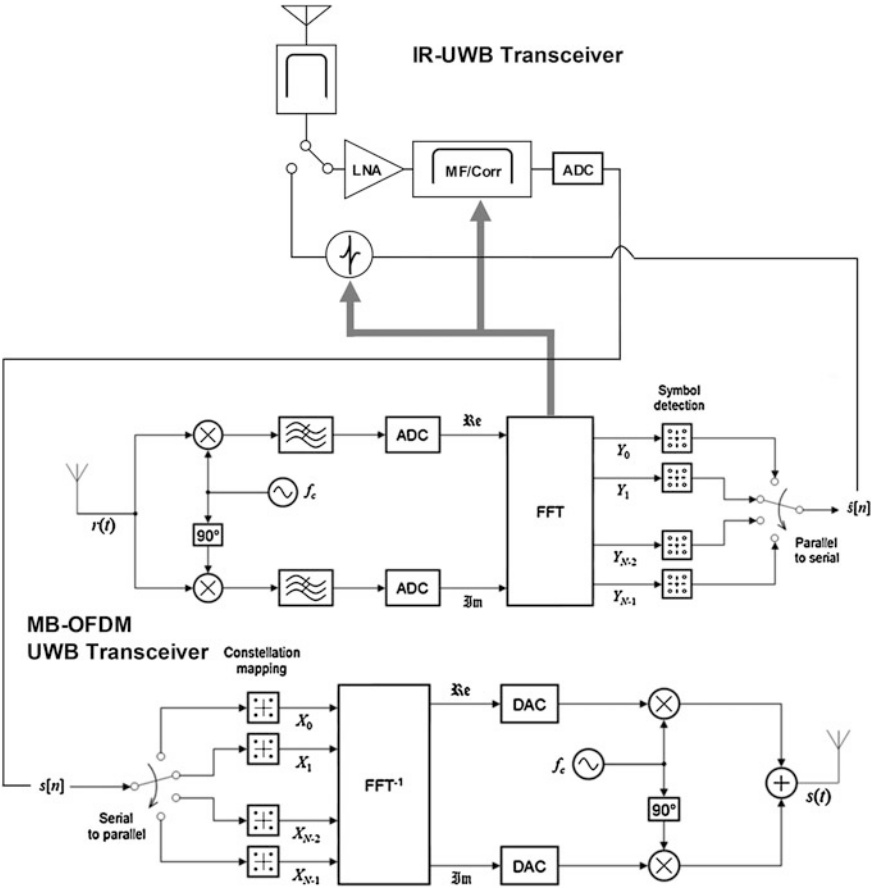

Fig. 6.13 Architecture of a BNC performing the role of a CRC for MBAN by using UWB technology. The *bold arrows* indicate the flow of information on spectrum availability from the MB-OFDM UWB transceiver to the IR-UWB transceiver

parameters of the CR clients (i.e., wearable sensors) for wireless access. The wearable sensors must be low cost, small in size, and with low power dissipation; this can be achieved through the use of an IR-UWB radio interface for communications in the first communications tier (see Fig. 6.9). Hence, the communication links between the sensors and the BNC should be implemented with IR-UWB as specified by IEEE 802.15.6. On the other hand, for the connection of the BNC with the second communication tier, the MB-OFDM-based ECMA-368 interface [35] should be used. Besides supporting high data rates, MB-OFDM technology also provides a relatively straightforward way to implement detect-and-avoid (DAA) and CR features.

Figure 6.13 shows the architecture for a UWB-BAN CRC, consisting of two transceivers, an IR-UWB transceiver with on–off keying (OOK) modulation and a

Layout: T1 Standard SC | Book ID: 318863_1_En | Book ISBN: 978-3-319-04021-9
Chapter No.: 6 | Date: 24-12-2013 | Page: 27/40

MB-OFDM UWB transceiver. The division of the 3.1–10.6 GHz UWB spectrum into 14 sub-bands of 528 MHz as suggested by the ECMA-368 standard can be adopted. The lower UWB frequency band (3.1–4.8 GHz) is then covered by three sub-bands with center frequencies at 3232, 3960, and 4488 MHz, respectively. Due to better propagation characteristics, these three sub-bands should be preferred for first-tier communications. The second-tier communications can be implemented in higher frequencies.

The fast Fourier transform (FFT) engine monitors the UWB spectrum and broadcasts information on available sub-bands for data transmission. It has been demonstrated that the 128-bin FFT engine of the OFDM transceiver can act as a rudimentary spectrum analyzer with a sampling frequency of 528 MHz resulting in a frequency resolution of 4.125 MHz (528 MHz/128 bins) [36]. This enables the estimation of spectrum occupancy for opportunistic spectrum usage purposes with minimal additional implementation costs. A MB-OFDM transceiver also facilitates the protection of sensitive receivers or protected medical devices from UWB interference by using frequency-domain spectrum shaping. This can be achieved by zeroing a range of subcarriers that overlap with the frequency band one intends to protect during transmission.

The broadcast channel is one of the three sub-bands of the lower UWB frequency band, which is chosen based on spectrum usage statistics. The least congested frequency sub-band is the most convenient choice for the broadcast channel and this information is stored in the memory of each of the sensor nodes and the CNC. When a wearable sensor is turned on, the device is informed (through the broadcast channel) of which sub-band it can use for data transmission. Then, it adapts accordingly the matched filter (MF) of the correlator in the receiver and the pulse generator of the transmitter. The same is done in the IR-UWB transceiver of the CNC. This can be implemented through a simple look-up table for the MF and pulse generator.

6.3.2.6 Cognitive Radio and Energy Consumption

Energy consumption is an important issue for BANs and elements therein, particularly for communications at the first tier of operation (Fig. 6.9). Energy efficiency facilitates operation for the user through reducing frequency of battery charges whereby the user may find it difficult to carry out such tasks due to his or her current condition. It also improves reliability through reducing the probability of the network or the sensors therein being rendered inoperable due to energy depletion.

BANs employ a range of means to reduce communications energy consumption [37]. CR is also highly pertinent to energy saving in BANs through at least two key means. The first is better dynamic selection of spectrum, avoiding interference and therefore reducing necessary received power hence transmitted power. MB-OFDM-based UWB leaves scope to tailor transmissions towards the lowest interference spectrum.

The second energy-saving advantage of using CR involves the use of cognition to achieve better awareness of context, including higher-layer communication

requirements, the changing general environment, and the battery energy level. This awareness can be used to improve timing of transmissions and dynamic MAC and physical (PHY) positioning given the current and projected interference conditions, variations in required data rates and constraints such as delay, and variations in general channel conditions and sensor energy availability. For example, BAN sensor readings such as blood pressure, oxygen saturation, and blood sugar levels might be sampled at changing intervals and rates, depending on the condition of the patient and time of day. In order to dynamically maintain the appropriate configuration of the BAN communication with minimized outage due to battery energy depletion while still aiming to communicate all data with appropriate delay constraints, learning and cognition can play a key part in estimating the future in terms of how requirements for these readings and battery levels are likely to vary. This can be matched to sensor transmission timing, rate, and MAC/PHY characteristics dependent on battery conditions. Moreover, battery conditions might also be driven by energy harvesting as it is described later in this section. Learning and prediction of such increases is also a key use for cognition, particularly given that the temporal characteristics of such incoming charge are highly dependent on the specific patient's nature.

6.3.3 Wireless Body Area Networks

6.3.3.1 Introduction

In the context of WBANs, electromagnetic RF energy harvesting is valuable and could be accomplished by using wearable antennas that allow for power supplying the sensor nodes [38]. Ubiquitously available RF sources, operating at different bands, are therefore exploited for RF electromagnetic energy harvesting purposes.

In this section, the opportunistic radio frequency bands for RF energy harvesting have been identified. Moreover, based on power density measurements, we have been able to identify the best spectrum opportunities that may be considered in order to conceive multiband antennas for electromagnetic energy harvesting. As an example of energy harvesting implementation, the readers are directed to familiarise with the RF energy harvesting system developed in the context of the PROENERGY-WSN project [39], which consists of an impedance matching circuit, rectifier and the energy storage sub-system.

6.3.3.2 Indoor and Outdoor RF Energy Harvesting Opportunities

In order to seek the best spectrum opportunities for RF energy harvesting, several field trial measurements have been conducted in Covilhã, Portugal, by using the NARDA-SMR spectrum analyser with a measuring antenna, in both indoor and outdoor environments.

Fig. 6.14 Locations of the measurements in Covilhã, Portugal

(A) Average Received Power

By analysing the power density measurements in 36 different locations, we intend to find the best frequencies for RF energy harvesting. Besides, the identified spectrum opportunities are being considered to conceive multi-band antennas. The location for the measurements is shown in Fig. 6.14. To determine the received power, Pr, of the spectrum analyser, we multiply the power density, Pd, by the effective receiving area of the antenna, Ae, and gain, G = 1, as follows:

$$p_d\left[W/m^2\right] = \left|E^2\right|/(120.\pi) \tag{6.3.5}$$

$$\overline{P_r[dBm]} = 10 \cdot \log\left(P_d \frac{\lambda^2 \cdot G}{4\pi}\right) + 30 \tag{6.3.6}$$

where E is the electric field and λ is the wavelength.

To choose the best frequency bands for electromagnetic energy harvesting, we have determined the average of each of the n values of the received power, P_{ri} [W] in linear units, in five different locations, where n is the number of measurements taken, for each frequency. The average received power, in dBm, was then calculated as follows:

$$\overline{P_r[dBm]} = 10 \cdot \log\left(\frac{\sum_{i=1}^{n} P_{ri}[W]}{n}\right) + 30 \tag{6.3.7}$$

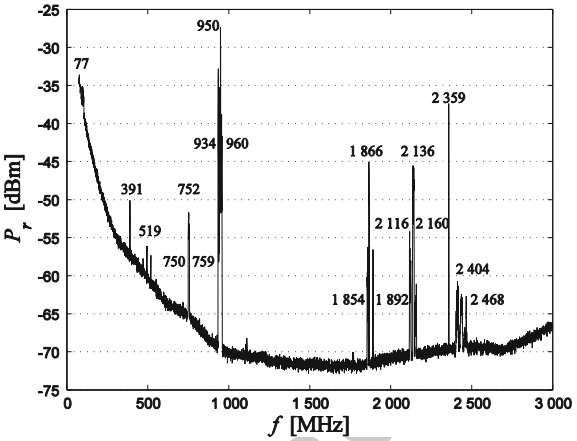

Fig. 6.15 Average received power as a function of the frequency for the university scenario (indoor)

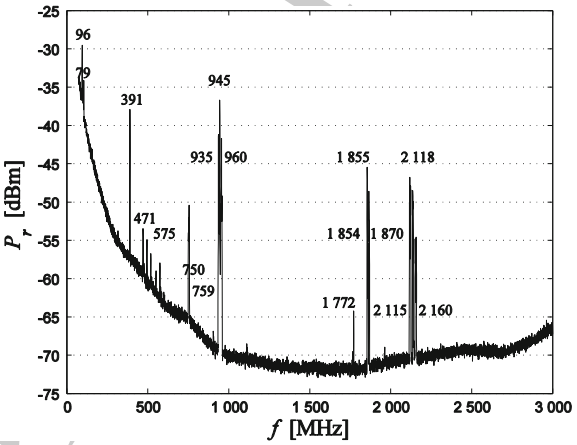

Fig. 6.16 Average received power for the outdoor scenario

(B) Indoor Opportunities

Figure 6.15 presents the indoor spectrum opportunities as observed at the higher education institution in Covilhã.

The set of frequencies with high energy available for harvesting comprises the range from 934 to 960 MHz (GSM900), 1854 to 1892 MHz (GSM1800), 2116 to 2160 MHz (UMTS), 2359 MHz (amateur, SAP/SAB applications, video), and 2404 to 2468 MHz (Wi-Fi).

(C) Outdoor Opportunities

The location of public places in the outdoor scenario for the field trial results were identified in Fig. 6.14 as locations numbered 8, 9, 12, 13, 14, 21 and 22. The corresponding values of the average received power are shown in Fig. 6.16.

The set of frequencies with more energy available for harvesting are in the range from 79 to 96 MHz (mobile/radio broadcast stations), 391 MHz (emergency

Layout: T1 Standard SC | Book ID: 318863_1_En | Book ISBN: 978-3-319-04021-9
Chapter No.: 6 | Date: 24-12-2013 | Page: 31/40

broadcast stations), 750 to 759 MHz (digital television broadcast stations), 935 to 960 MHz (GSM 900 broadcast stations), 1854 to 1870 MHz (GSM 1800 broadcast stations) and 2115 to 2160 MHz (UMTS broadcast stations).

It may be concluded from the above reported measurements that the GSM900/1800 frequency bands appear to be the most promising bands for RF energy harvesting.

6.3.3.3 Innovative MAC Protocols

In [40] the authors have shown that one fundamental reason for IEEE 802.15.4/4a MAC inefficiency is overhead, where the use of ACK control packets can decrease the bandwidth efficiency about 10 %. In this work, we propose and analyse two innovative mechanisms to reduce overhead in IEEE 802.15.4: (1) concatenation and (2) piggyback [41]. The main idea is to improve channel efficiency by aggregating several acknowledgment (ACK) responses into one single transmission (i.e., one single packet) like in the IEEE 802.11e standard. This aggregation of ACKs aims at reducing the overhead by transmitting less ACK control packets and by decreasing the time periods the transceivers should switch between different states.

We aim at increasing the throughput as well as decreasing the end-to-end delay, whilst providing a feedback mechanism for the receiver to inform the sender about how many transmitted (TX) packets were successfully received (RX). Our proposal also considers the use of the Request-To-Send/Clear-To-Send (RTS/CTS) mechanism, in order to avoid the hidden terminal problem.

In IEEE 802.15.4 the protocol overhead impacts on end to-end delay and throughput. In order to reduce end-to-end delay and increase throughput, we propose a new innovative MAC protocol that solves the above problems, along with the elimination of the backoff period repetitions, the Sensor Block Acknowledgment (SBACK)-MAC protocol [42]. The main difference compared to IEEE 802.15.4 is related to the way that SBACK-MAC treats the ACK control packets. The SBACK-MAC allows the aggregation of several ACK responses into one special packet. The *BACK Response* will be responsible to confirm a set of data packets successfully delivered to the destination. This packet has the same length as an ACK packet in IEEE 802.15.4. Hence, an ACK control packet will not be received in response to every data packet sent/received. By decreasing the number of control packets exchanged in a wireless medium, it is possible to decrease not only the number of collisions but also the number of back-off periods (the time a node must wait before attempting to transmit/retransmit the packet) on each node. Moreover, in WSNs the length of control packets can be of the order of magnitude of the data packets. Since nodes are battery operated, the transmission of such packets leads to energy decrease, whilst reducing the number of data packets that will be transmitted containing useful information (i.e., goodput).

The SBACK-MAC also considers the *ccaTime*. This way, during CCA nodes are able to determine the channel state (i.e., busy or idle), which allows for providing statistical information for the MAC sub-layer and upper layers.

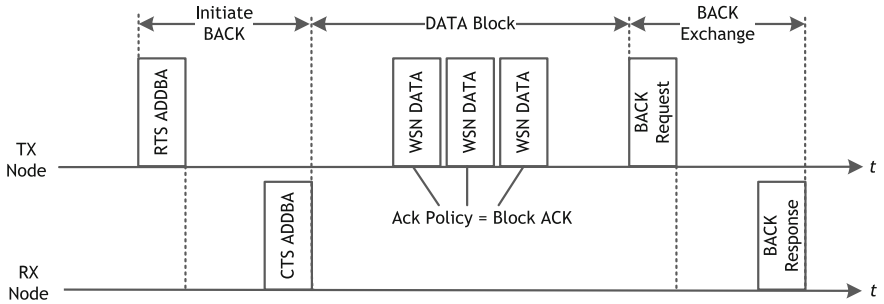

Fig. 6.17 SBACK-MAC protocol—block acknowledgment mechanism with *BACK request*

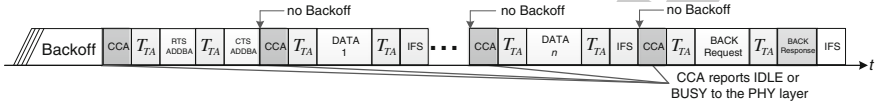

Fig. 6.18 Frame sequence for the SBACK-MAC protocol with BACK request (concatenation)

Moreover, since the CCA result is based on the obtained Received Signal Strength Indicator (RSSI), transmission power control techniques could be used to estimate the minimum transmission power for sending each packet to a neighbouring node.

(A) Block Acknowledgment Mechanism with BACK Request

The version of the proposed SBACK-MAC protocol with *BACK Request* considers the exchange of two special packets, i.e., *RTS ADDBA* and *CTS ADDBA*, where *ADDBA* stands for "Add Block Acknowledgement". After this successfully exchange, data packets are transmitted from the transmitter to the receiver (e.g., 100 packets are sent during the active periods). Afterwards, by using the BACK Request primitive, the transmitter inquires the receiver about the total number of data packets that successfully reach the destination. In response, the receiver will send a special data packet, called BACK Response identifying the packets that require retransmission, and the BACK mechanism finishes.

Figure 6.17 presents the message sequence chart for the BACK mechanism.

The exchange of two types of special control packets used at beginning and end of the BACK mechanism allows for mitigating the hidden-terminal and exposed-terminal problems like in IEEE 802.11e. The BACK mechanism also aims at reducing the power consumption by transmitting less ACK control packets and by decreasing the time periods the transceivers should switch between different states. By using the BACK there is no need to receive an ACK for every DATA packet sent, as presented in Fig. 6.18. Besides, during the data transmission there is no way to know how many packets have successfully reached the destination, except at the end of communication by using the *BACK Request/BACK Response* (we set, *BE*, equal to 0), as if there is no congestion.

Table 6.1 IEEE 802.15.4 and SBACK-MAC typical parameters and values

Description	Symbol	Value
Backoff period duration	T_{BO}	320 μs
PHY SHR duration	T_{SHR}	160 μs
CCA detection time	T_{CCA}	128 μs
TX/RX or RX/TX switching time	T_{TA}	192 μs
Short interframe spacing (SIFS) time	T_{SIFS}	192 μs
Long interframe spacing (LIFS) time	T_{LIFS}	640 μs
ACK transmission time	T_{ACK}	352 μs
RTS transmission time	T_{RTS}	352 μs
CTS transmission time	T_{CTS}	352 μs
RTS ADDBA transmission time	T_{RTS_ADDBA}	352 μs
CTS ADDBA transmission time	T_{CTS_ADDBA}	352 μs
BACK request transmission time	$T_{BRequest}$	352 μs
BACK response transmission time	$T_{BResponse}$	352 μs
ACK wait duration time	T_{AW}	560 μs
DATA transmission time	T_{DATA}	576 μs
Time to setup radio to RX or TX states	rxSetupTime	1792 μs
PHY length overhead	L_{H_PHY}	6 bytes
MAC overhead	L_{H_MAC}	9 bytes
DATA payload	L_{H_DATA}	3 bytes
DATA frame length	L_{FL}	18 bytes
ACK/RTS/CTS frame length	L_{ACK}	11 bytes
Number of TX frames	n	1 to 100
Data rate	R	250 kb/s

When the SBACK-MAC with *BACK Request* is considered, the minimum average delay, $D_{\min}$, in seconds, is given by:

$$D_{\min\_\mathrm{BACK}} = \left(\overline{CW} + ccaTime + T_{RTS_{ADDBA}} + H_1\right)/n \tag{6.3.8}$$

where $H_1 = T_{TA} + T_{CTS\_ADDBA} + n \times (ccaTime + T_{TA} + T_{DATA} + T_{TA} + T_{IFS}) + ccaTime + T_{TA} + T_{BRequest} + T_{TA} + T_{BResponse} + T_{IFS}$.

The maximum average throughput, $S_{\max}$, in bits per second, is given by:

$$S_{\max\_\mathrm{BACK}} = 8L_{DATA}/D_{\min\_\mathrm{BACK}} \tag{6.3.9}$$

The meaning of the parameters is defined in Table 6.1.

By analysing Eqs. (6.3.8) and (6.3.9), we conclude that by using the *BACK Request* primitive we allow several MAC Protocol Data Units (MPDUs) to be acknowledged by a single *BACK Request* packet. Therefore, compared with IEEE 802.15.4 in the basic access mode, there is no need to consider the use of individual ACK control packets. We also assume that the back-off period is equal to 0, as if there is no congestion (no activity in the shared medium). This is explained by the fact that a CTS can be only sent if there is no congestion at the receiver. The *BACK Response* contains the information about the reception of corresponding MPDUs by using a specific bitmap that is transmitted as an answer to an explicit

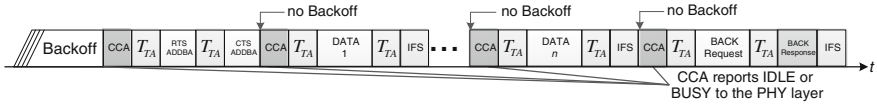

Fig. 6.19 Frame sequence for the SBACK-MAC protocol with no *BACK request* (piggyback)

transmitter request. This request is performed by the new *BACK Request* control frame. Both the *BACK Request* and *BACK Response* are transmitted at the same data rate (i.e., 250 kb/s).

(B) Proposed scheme with no BACK Request

The version of the SBACK-MAC protocol with no *BACK Request* ("piggyback mechanism") also considers the exchange of the *RTS ADDBA* and *CTS ADDBA* packets at the beginning of the communication. However, at the end of the communication the BACK Request primitive is not transmitted. Therefore, the last aggregated data frame must include the information about the packets previously transmitted, as shown in Fig. 6.19.

The SBACK-MAC version with "piggyback" does not consider the use of the BACK Request primitive, as shown in Fig. 6.19. As a consequence the control overhead and the end-to-end delay are reduced whilst increasing the throughput, by piggybacking the BACK information into the last data fragment. However, with this scheme, the system becomes less robust. If the last aggregated frame (DATA frame n) is lost, the destination does not know that an ACK needs to be sent back.

When the SBACK-MAC with no *BACK Request* is considered, the minimum average delay, $D_{\min\_\text{Piggy}}$, in seconds, is given by:

$$D_{\min\_\text{Piggy}} = \left(\overline{CW} + ccaTime + T_{RTS_{ADDBA}} + H_2\right)/n \tag{6.3.10}$$

where $$H_2 = T_{TA} + T_{CTS\_ADDBA} + (n-1) \times (ccaTime + T_{TA} + T_{DATA} + T_{TA} + T_{IFS}) + ccaTime + T_{TA} + T_{DATA} + T_{TA} + T_{B\text{Response}} + T_{IFS}$$

The maximum average throughput, $S_{\max\_\text{Piggy}}$, in bits per second, is given by:

$$S_{\max\_\text{Piggy}} = 8L_{DATA}/D_{\min\_\text{Piggy}} \tag{6.3.11}$$

The meaning of the parameters is defined in Table 6.1.

By analysing Eqs. (6.3.10) and (6.3.11), we conclude that in the SBACK-MAC with no BACK Request, (n-1) frames are transmitted (which corresponds to less one IFS) like in the SBACK-MAC with *BACK Request*. However, since the last data packet includes the information about the total number of packets previously transmitted, the *BACK Response* is transmitted immediately after the reception of the last data frame. Therefore, there is no need to transmit the *BACK Request* packet.

(C) Modelling and simulation results

The SBACK-MAC was evaluated by using the MiXiM simulation framework [36] from the OMNeT++ simulator. SBACKMAC throughput and end-to-end delay with and with no *BACK Request* have been compared against IEEE

Layout: T1 Standard SC | Book ID: 318863_1_En | Book ISBN: 978-3-319-04021-9
Chapter No.: 6 | Date: 24-12-2013 | Page: 35/40

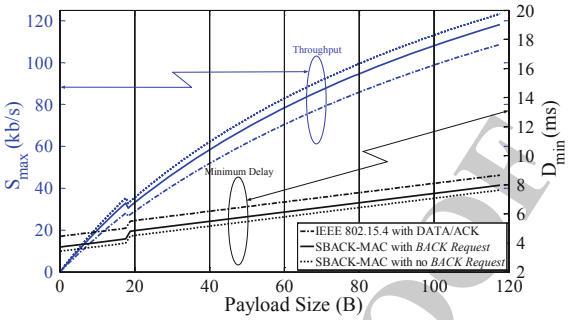

Fig. 6.20 Maximum throughput and minimum delay versus payload size

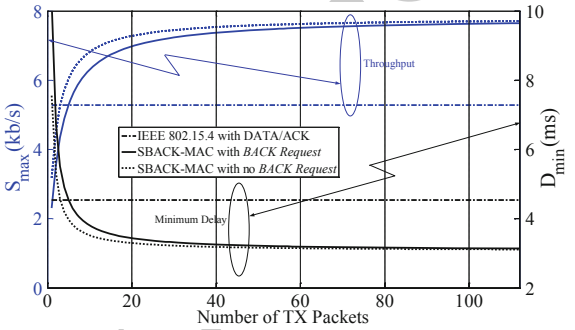

Fig. 6.21 Maximum throughput and minimum delay versus number of TX packets

802.15.4, by considering a 95 % confidence interval, however, as it is too small, we decided not to plot it in the figures. Table 6.1 presents the MAC parameters considered for the network in our simulations. The performance analysis of the proposed schemes is conducted for the best-case scenario. Therefore, we are assuming that the channel is an ideal channel, with no transmission errors. During the active period, there is only one node that always has a frame to be sent. The other stations can only accept frames and provide acknowledgments.

Figure 6.20 presents the maximum average throughput and the minimum average delay versus the payload size for the SBACK-MAC protocol with and with no *BACK Request*. The discontinuity around 18 bytes is due to the use of SIFS and LIFS (i.e., MPDU less of equal than 18 bytes must be followed by a SIFS, whilst MPDU longer than 18 bytes must be followed by a LIFS). The number of transmitted frames, n, is 10 (i.e., for the SBACK-MAC, the frames are aggregated and transmitted in a burst).

It is observed that, by increasing the payload size, S_{max} also increases. This conclusion is valid for all the three presented mechanisms. For small packet sizes (i.e., data payload less or equal than 18 bytes) by comparing the IEEE 802.15.4 with the SBACK-MAC protocol, with and with no *BACK Request*, S_{max} increases 17 % and 25 %, respectively. Moreover, by using the IEEE 802.15.4 basic access mode with DATA/ACK, the maximum achievable throughput is approximately 108.7 kb/s whereas, by using the SBACK-MAC with and with no *BACK Request*,

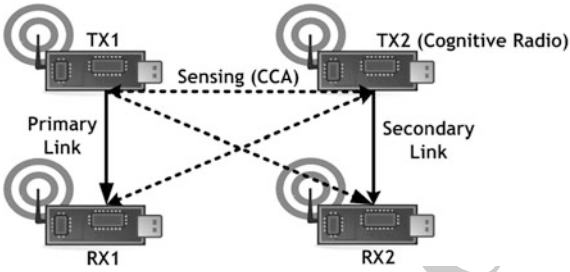

Fig. 6.22 Signal and interference paths in a cognitive radio sensor network

the maximum achievable throughput is 118.1 and 123.2 kb/s, respectively. Results for D_{min} as a function of the payload size show that, by using SBACK-MAC with and with no *BACK Request* for small packets sizes (i.e., data payload less or equal to 18 bytes), D_{min} decreases 17 and 25 %, respectively. For larger packet sizes, by considering SBACK-MAC with and with no *BACK Request*, D_{min} decreases by 8 and 13 %, respectively.

Figure 6.21 presents S_{max} and D_{min} as a function of the number of TX packets. A fixed payload size of 3 bytes (i.e., LDAT A = 3 bytes) is considered, since it is one of the values in the range from 1 to 18 bytes presented in Fig. 6.20, by considering the worst throughput performance, when taking into account the BACK mechanism. Even for the shortest payload sizes, it is possible to improve the network performance by using the proposed BACK mechanisms.

It may be observed that when the number of TX packets is less than 4, the IEEE 802.15.4 standard through the basic access mode, achieves higher throughput in comparison to SBACK-MAC (either with or with no *BACK Request*). Moreover, by considering the IEEE 802.15.4 standard in the basic access mode, S_{max} does not depend on the number of TX packets, and achieve the maximum value of 5.2 kb/s. In SBACK-MAC with and with no *BACK Request* (i.e., concatenation and piggyback), S_{max} increases by increasing the number of TX packets (i.e., the number of aggregated packets). For a number of TX packets equal to 18, by considering the SBACK-MAC with *BACK Request* (i.e., concatenation version) S_{max} is about 6.3 kb/s. This value corresponds to an increase of 21 % in the throughput in comparison to the MAC protocol from the IEEE 802.15.4 standard in the basic access mode, whereas by considering the SBACK-MAC with no *BACK Request* (i.e., piggyback version), the achievable throughput is 6.8 kb/s, an increase of 30 %. However, the difference on the throughput between the SBACK-MAC with and with no *BACK Request* tends to decrease by increasing the total number of TX packets (i.e., by aggregating more packets). We also conclude that, for more than 4 TX packets, SBACKMAC (with and with no *BACK Request*) delay is significantly shorter than for IEEE 802.15.4 in the basic access mode. The difference is mitigated by increasing the total number of TX packets (i.e., by aggregating more packets).

The previous results have shown that the use of the proposed BACK mechanisms enables to improve the network performance whilst increasing the channel

Layout: T1 Standard SC | Book ID: 318863_1_En | Book ISBN: 978-3-319-04021-9
Chapter No.: 6 | Date: 24-12-2013 | Page: 37/40

use optimization. Therefore in the context of cognitive radio wireless sensor networks (CRWSN) the proposed BACK mechanisms can be applied in a scenario where the secondary user's flow alternates between sensing (i.e., CCA mechanism) and sending rapidly at short intervals [43], see Fig. 6.22.

By considering that the primary user data flow (from TX_1 to RX_1) is bursty, there will be inactive periods between transmissions. These inactive periods are used by the secondary users to send their own traffic. Since, by using the proposed BACK mechanism we decrease the end-to-end delay whilst increasing throughput we intend to exploit the temporal opportunities (i.e., temporal "white spaces") [43] more efficiently, by decreasing the transmissions times of secondary users. Moreover, CRWSN nodes must perform sensing and make a decision about the channel state (i.e., busy or idle). This spectrum decision time can also be seen has overhead, leading to an increase of the energy consumption. Therefore, in the case of re-transmissions, the SBACK-MAC protocol with and with no *BACK Request*, is able to decrease the time periods before making CCA again, since there is no back-off phase between two consecutive data packets, which allows for decreasing the total overhead.

6.3.3.4 Summary and Conclusions

We have identified the spectrum opportunities for RF energy harvesting to power supply the wireless sensor nodes in real indoor/outdoor scenarios. The set of indoor/outdoor most promising frequency bands are 79–96 MHz (mobile/radio broadcast stations), 391 MHz (emergency broadcast stations), 750–758 MHz (digital television broadcast stations), 935–960 MHz (GSM 900 broadcast stations), 1855–1868 MHz (GSM 1800 broadcast stations) and 2115–2160 MHz (UMTS broadcast stations). A scenario of using RF harvesting with dedicated devices had been analysed in the PROENERGY-WSN [39]. It enables future WBAN to operate without the need of replacing batteries. Moreover, in order to reduce the overhead that affects WBANs communications we have proposed SBACK-MAC—a new contention-based MAC protocol that uses a BACK mechanism to improve channel efficiency by aggregating several ACK into one special packet, the *BACK Response*. By using a concatenation mechanism the total overhead is decreased, since there is no back-off between two consecutive data packets. Two innovative solutions have been proposed to improve the IEEE 802.15.4 performance. The first one considers the SBACK-MAC protocol in the presence of *BACK Request* (concatenation mechanism), while the second considers the SBACK-MAC in the absence of BACK Request (piggyback mechanism).

6.3.4 Conclusions

The growing use of radio communication technology for healthcare is triggering the deployment of BANs in medical premises mostly on a license-exempt

secondary basis. This fact motivates further studies on interference mitigation techniques for medical communication environments. CR offers viable cost-effective and future-proof solutions addressing both scalability and coexistence issues.

The next generation of CR networks will be supplied by renewable energy from natural resources, where RF energy harvesting plays an important role. In a near future, RF energy will enable to power supply all the nodes without the need of replacement of the primary source of energy (i.e., batteries).

In order to improve the efficiency of WBANs, a new innovative Sensor Block Acknowledgment (SBACK)-MAC protocol which aggregates several ACK responses into one special packet has been proposed. The results presented here show that the proposed concatenation mechanisms considerably improve network performance in terms of throughput and end-to-end delay. In the context of CR wireless sensor networks enhancements will be achieved because of the reduction of queue lengths of secondary users as well as the channel utilisation.

Dynamic spectrum access can be used to mitigate spectrum scarcity. This is accomplished by enabling an unlicensed user (i.e., secondary user) to adaptively adjust its operating parameters and exploit the spectrum which is unused by licensed users (i.e., primary users), in an opportunistic manner.

References

1. ITU Final Acts of the Regional Radiocommunication Conference for planning of the digital terrestrial broadcasting service in parts of Regions 1 and 3, in the frequency bands 174–230 MHz and 470–862 MHz (RRC-06), International Telecommunication Union, Geneva, 2006
2. Więcek, D.: Methodology of White Space estimation in TV bands based on the ITU GE06 technical conditions, COST IC0905 TERRA 3rd Workshop, Brussels, 21st June 2011
3. ECC Report 185, Complementary Report to ECC Report 159. Further definition of technical and operational requirements for the operation of white space devices in the band 470–790 MHz, ECC, 2013
4. ITU-R, Recommendation P.1546-4 Method for point-to-area predictions for terrestrial services in the frequency range 30–300 MHz. International Telecommunication Union, Geneva, October 2009
5. WISE, http://wise.turkuamk.fi, cited 31.5.2013
6. Tekes Trial Programme, http://www.tekes.fi/programmes/Trial, cited 31.5.2013
7. ECC report 159, Technical and operational requirements for the possible operation of CR systems in the 'white spaces' of the frequency band 470–790 MHz, January 2011
8. ITU-R Document 6E/64-E, The ESR5 criterion for the Assessment of DVB-T transmission Quality, April 2004
9. Talmola, P., Kalliovaara, J., Paavola, J., Ekman, R., Kokkinen, H., Heiska, K., Wichman, R., Poikonen, J.: Field measurements of WSD-DTT protection ratios over outdoor and indoor reference geometries. In: Proceedings of International Conference on Cognitive Radio Oriented Wireless Networks CROWNCOM 2012, Stockholm, Sweden, 2012
10. CEPT/ECC SE 43(11)36 WISE Project Measurement Report, WSD maximum Power Measurements in Turku Test Network, 10th SE43 meeting, Bologna, Italy, July 2011

AQ3

Layout: T1 Standard SC | Book ID: 318863_1_En | Book ISBN: 978-3-319-04021-9
Chapter No.: 6 | Date: 24-12-2013 | Page: 39/40

11. CEPT/ECC SE43(11)81 WISE Project Measurement Report, WSD maximum Power Indoor Measurements in Turku Test Network, 12th SE43 meeting, Cambridge, UK, December 2011
12. Ojaniemi, J., Poikonen, J., Wichman, R.: Effect of geolocation database update algorithms to the use of TV white spaces. In: Proceedings of International Conference on Cognitive Radio Oriented Wireless Networks CROWNCOM 2012, Stockholm, Sweden, 2012
13. Ojaniemi, J., Kalliovaara, J., Alam, A., Poikonen, J., Wichman, R.: Optimal field measurement design for radio environment mapping. In: Proceedings of 47th Annual Conference on Information Sciences and Systems (CISS 2013)
14. CEPT/ECC SE43(11)82 WISE Project Measurement Report, PMSE protection measurements in Helsinki City Theatre. 12th SE43 meeting, Cambridge, UK, December 2011
15. Radio Standards Specifications (RSS-Gen, RSS-210, RSS-310), Procedures and regulations. http://www.ic.gc.ca/eic/site/smt-gst.nsf/eng/h_sf01841.html
16. FCC Part-15 and FCC Part-18 rules, http://www.fcc.gov
17. Enhancing the Security of Corporate Wi-Fi Networks Using DAIR. Paramvir Bahl et al. MobiSys'06, June 19–22, 2006, Uppsala, Sweden
18. Flores, A.B., Guerra, R.E., Knightly, E.W., Ecclesine, P., Pandey, S.: IEEE 802.11af: a standard for TV white space spectrum sharing. IEEE Commun. Mag. 51(10), 92–100 (2013)
19. van Bloem, J.W.H., Schiphorst, R., Kluwer, T., Slump, C.H.: Spectrum utilization and congestion of IEEE 802.11 networks in the 2.4 GHz ISM band. J. Green Eng. 2(4), 401–430 (2012). ISSN 1904-4720
20. Nardelli, B., Lee, J.,Lee, K., Yi, Y., Chong, S., Knightly, E.W., Chiang, M.: Experimental evaluation of optimal CSMA. In: INFOCOM, 2011 Proceedings IEEE, pp. 1188–1196, 10–15 April 2011
21. Alemdar, H., Ersoy, C.: Wireless sensor networks for healthcare: a survey. Comput. Netw. **54**(15), 2688–2710 (2010)
22. Jovanov, E., Milenkovic, A.: Body area networks for ubiquitous healthcare applications: opportunities and challenges. J. Med. Syst. **35**(5), 1245–1254 (2011)
23. IEEE Standard for Local and Metropolitan Area Networks–Part 15.6: Wireless Body Area Networks, IEEE Standard 802.15.6-2012, 2012
24. Cao, H., Leung, V., Chow, C., Chan, H.: Enabling technologies for wireless body area networks: a survey and outlook. IEEE Commun. Mag. **47**(12), 84–93 (2009)
25. Hauer, J.-H., Handziski, V., Wolisz, A.: Experimental study of the impact of WLAN interference on IEEE 802.15.4 body area networks. Wireless Sens. Netw. **5432**, 17–32 (2009)
26. Chávez-Santiago, R., Khaleghi, A., Balasingham, I., Ramstad, T.A.: Architecture of an ultra wideband wireless body area network for medical applications. In: Proceedings of 2nd International Symposium on Applied Sciences in Biomedical and Communication Technologies (ISABEL), Bratislava, Slovak Republic, November 24–27, 2009, pp. 1–6
27. Wang, J., Gosh, M., Chan, H.: Emerging cognitive radio applications: a survey. IEEE Commun. Mag. **49**(3), 74–81 (2011)
28. Jabbar, H., Song, Y.S., Jeong, T.T.: RF energy harvesting system and circuits for charging of mobile devices. IEEE Trans. Consum. Electron. **56**(1), 247–253 (2010)
29. Barroca, N., Ferro, J.M., Borges, L.M., Tavares, J., Velez, F.J.: Electromagnetic energy harvesting for wireless body area networks with cognitive radio capabilities. In: Proceedings of URSI Seminar of the Portuguese Committee, Lisbon, Portugal, November 2012
30. Cotton, S.L., Scanlon, W.G.: Characterization and modeling of the indoor radio channel at 868 MHz for a mobile bodyworn wireless personal area network. IEEE Antennas Wireless Propag. Lett. **6**(1), 51–55 (2007)
31. Doost-Mohammady, R., Chowdhury, K.R.: Transforming healthcare and medical telemetry through cognitive radio networks. IEEE Wireless Commun. **19**(4), 67–73 (2012)
32. Phunchongharn, P., Hossain, E., Niyato, D., Carmolinga, S.: A cognitive radio system for e-health applications in a hospital environment. IEEE Wireless Commun. **17**(1), 20–28 (2010)
33. Chávez-Santiago, R., et al.: Cognitive radio for medical body area networks using ultra wideband. IEEE Wireless Commun. **19**(4), 74–81 (2012)

Layout: T1 Standard SC | Book ID: 318863_1_En | Book ISBN: 978-3-319-04021-9
Chapter No.: 6 | Date: 24-12-2013 | Page: 40/40

34. Chávez-Santiago, R., Jankūnas, D., Fomin, V.V., Balasingham, I.: A dual-band MAC protocol for indoor cognitive radio networks: an e-health case study. In: Proceedings of 8th International Conference on Body Area Networks (BodyNets), Boston, MA, September 30–October 2, 2013
35. High Rate Ultra Wideband PHY and MAC Standard, ECMA-368 Standard, December 2008
36. Batra, A., Lingam, S., Balakrishman, J.: Multi-band OFDM: a cognitive radio for UWB. In: Proceedings of IEEE International Symposium on Circuits Systems (ISCAS), Island of Kos, Greece, May 21–24, 2006, pp. 4094–4097
37. Chen, M., Gonzalez, S., Vasilakos, A., Cao, H., Leung, V.C.M.: Body area networks: a survey. Mob. Netw. Appl. J. **16**(2), 171–193 (2011)
38. Bellon, J.S., Cabedo-Fabres, M., Antonino-Daviu, E., Ferrando-Bataller, M., Penaran-da-Foix, F.: Textile MIMO antenna for wireless body area networks. In: Proceedings of the 5th European Conference on Antennas and Propagation (EUCAP), Rome, Italy, April 2011, pp. 428–432
39. PROENERGY-WSN, Prototypes for Efficient Energy Self-sustainable Wireless Sensor Networks. http://www.e-projects.ubi.pt/proenergy-wsn, Apr. 2013
40. Chowdhury, M.S., Ullah, N., Kabir, Md.H., Khan, P., Kwak, K.S.: Throughput, Delay and Bandwidth Efficiency of IEEE 802.15.4a Using CSS PHY. In: Proceedings of the International Conference on Information and Communication Technology Convergence (ICTC), Jeju Island, Korea 2010
41. IEEE Standard for Local and Metropolitan Area Networks–Part 15.4: Wireless Body Area Networks, IEEE Standard 802.15.4, 2011
42. Barroca, N., Velez, F.J., Chatzimisios, P.: Block acknowledgment mechanisms for the optimization of channel use in wireless sensor networks. In: Proceedings of the 24th Annual IEEE International Symposium on Personal, Indoor and Mobile Radio Communications (PIMRC 2013), London, UK, September 2013
43. Dash, D., Sabharwal, A.: Secondary transmission profile for a single-band cognitive interference channel. In: Proceedings of 42nd Asilomar Conference on Signals, Systems and Computers, Pacific Grove, California, USA, October 2008, pp. 1547–1551
44. ECC Report 185, Further definition of technical and operational requirements for the operation of white space devices in the band 470–790 MHz, January 2013
45. Distributed Sensing of Spectrum Occupancy and Interference in Outdoor 2.4 GHz Wi-Fi Networks. Salim Hanna, John Sydor. Globecom 2012, Dec 3–7 Anaheim, Calif
46. Tytgat, L., Barrie, M., Gonçalves, V., Yaron, O.Y., Moerman, I., Demeester, P., Pollin, S., Ballon, P., Delaere, S.: Techno-economical viability of cognitive solutions for a factory scenario. In: IEEE International Dynamic Spectrum Access Networks (DySPAN) Symposium (2011)
47. Barrie, M., Tytgat, L., Gonçalves, V., Yaron, O.Y., Moerman, I., Demeester, P., Pollin, S., Ballon, P., Delaere, S.: Techno-Economic Evaluation of Cognitive Radio in a Factory Scenario. Networking 2011 Workshop on Performance Evaluation of Cognitive Radio Networks: from Theory to Reality PE-CRN 2011, Springer LNCS book (2011)
48. Tytgat, L., Yaron, O., Pollin, S., Moerman, I., Demeester, P.: Avoiding collisions between IEEE 802.11 and IEEE 802.15.4 through coexistence aware clear channel assessment. EURASIP J. Wireless Commun. Netw. **2012**, 137 (2012). doi:10.1186/1687-1499-2012-137

Author Query Form

Book ID :	**318863_1_En**
Chapter No.:	**6**

Springer
the language of science

Please ensure you fill out your response to the queries raised below and return this form along with your corrections

Dear Author
During the process of typesetting your chapter, the following queries have arisen. Please check your typeset proof carefully against the queries listed below and mark the necessary changes either directly on the proof/online grid or in the 'Author's response' area provided below

Query Refs.	Details Required	Author's Response
AQ1	Please check and confirm that the authors and their respective affiliations have been correctly identified and also confirm corresponding author is correctly identified and amend if necessary.	
AQ2	Please confirm the section headings are correctly identified.	
AQ3	References [44–48] are given in list but not cited in text. Please cite in text or delete from list.	

MARKED PROOF

Please correct and return this set

Please use the proof correction marks shown below for all alterations and corrections. If you wish to return your proof by fax you should ensure that all amendments are written clearly in dark ink and are made well within the page margins.

Instruction to printer	*Textual mark*	*Marginal mark*
Leave unchanged	··· under matter to remain	
Insert in text the matter indicated in the margin		New matter followed by or
Delete	through single character, rule or underline or through all characters to be deleted	or
Substitute character or substitute part of one or more word(s)	through letter or through characters	new character or new characters
Change to italics	under matter to be changed	
Change to capitals	under matter to be changed	
Change to small capitals	under matter to be changed	
Change to bold type	under matter to be changed	
Change to bold italic	under matter to be changed	
Change to lower case	Encircle matter to be changed	
Change italic to upright type	(As above)	
Change bold to non-bold type	(As above)	
Insert 'superior' character	through character or where required	or under character e.g. or
Insert 'inferior' character	(As above)	over character e.g.
Insert full stop	(As above)	
Insert comma	(As above)	
Insert single quotation marks	(As above)	or and/or or
Insert double quotation marks	(As above)	or and/or or
Insert hyphen	(As above)	
Start new paragraph		
No new paragraph		
Transpose		
Close up	linking characters	
Insert or substitute space between characters or words	through character or where required	
Reduce space between characters or words	between characters or words affected	